REPUBLIC OF TURKEY
FIRAT UNIVERSITY
THE INSTITUTE OF NATURAL AND APPLIED SCIENCES
FACULTY OF SCIENCE

INVESTIGATION OF HEAT TREATMENT EFFECT ON PHYSICAL PROPERTIES OF Cu-Al-Ni-Nb QUATERNARY SHAPE MEMORY ALLOYS

Bahar Ali Mohammed FARAJ

Master's Thesis

Department of Physics

FEBRUARY - 2020

REPUBLIC OF TURKEY
FIRAT UNIVERSITY
THE INSTITUTE OF NATURAL AND APPLIED SCIENCES
FACULTY OF SCIENCE

Department of Physics

Master's Thesis

INVESTIGATION OF HEAT TREATMENT EFFECT ON PHYSICAL PROPERTIES OF Cu-Al-Ni-Nb QUATERNARY SHAPE MEMORY ALLOYS

Thesis Author

Bahar Ali Mohammed FARAJ

Supervisor: Assoc. Prof. Dr. Fethi DAĞDELEN

FEBRUARY – 2020

ELAZIĞ

REPUBLIC OF TURKEY
FIRAT UNIVERSITY
GRADUATE SCHOOL OF NATURAL AND APPLIED SCIENCES

Physics Department
Program: Solid State Physics

Master's Thesis

Title: Investigation of Heat Treatment Effect on Physical Properties Of Cu-Al-Ni-Nb Quaternary Shape Memory Alloys

Author: Bahar Ali Mohammed FARAJ

First Delivery: 30.12.2019

Date of Defense: 03.02.2020

THESIS APPROVAL

This thesis was prepared according to the rules of Firat University, Graduate School of Natural and Applied Sciences. It was evaluated by the jury members who have signed the following signatures and accepted unanimously because of the defense made available to the academic audiences.

Signature

Advisor: Assoc. Prof. Dr. Fethi DAGDELEN — I Approved
Firat University, Faculty of Science

Chairman: Assoc. Prof. Dr. Mediha KÖK — I Approved
Firat University, Faculty of Science

Member: Assist. Prof. Dr. Hasan BALLIKAYA — I Approved
Inonu University, OSB MYO

This thesis was registered at the meeting of the board of directors of the institute on

/ / 20

Signature

Prof. Dr. Soner ÖZGEN
Director of the Institute

ACKNOWLEDGEMENT

Cu-Al-Ni-based alloy is an important family of Cu-based shape memory alloys that investigated for some parameters. In this study time dependence aging was chosen as a heat treatment for Cu-Al-Ni-Nb SMAs. Some thermal and microstructural influnces has been studied.

I would like to thanks my supervisor, ***Associated Prof. Dr. Fethi Dagdelen*** to guide and advised me during this study. There is also my grateful to my teacher and my best friend, ***Associated Prof. Dr. Mediha KOK***, who encouraged me and teach me all supplementary subjects in my study.

Additionally, my parents who have gave me believe and supported me for whole of my life. Beside, many thanks for my husband, ***Ahmed Omer Ali Al-Jaf***, who supported me in all steps of my academic life. Also a special thanks for ***Mr. Ibrahim Nazem Qader***, for his scientific helps.

This work was supported by the Management Unit of the Scientific Research Projects of Firat University (FUBAP) (Project Numbers: FF.1906)

Bahar Ali Mohammed FARAJ
FEBRUARY -2020

TABLE OF CONTENTS

Page no

ABSTRACT

INVESTIGATION OF HEAT TREATMENT EFFECT ON PHYSICAL PROPERTIES OF Cu-Al-Ni-Nb QUATERNARY SHAPE MEMORY ALLOYS

Bahar Ali Mohammed FARAJ
Master Thesis
FIRAT UNIVERSITY
Graduate School of Natural and Applied Sciences
Department of Physics
February 2020, Pages: viii + 45

One of the important treatments that generally are using in industry and other fields of studies is heat treatment. Aging is a type of heat treatment that can be accomplished either with time dependence or temperature dependence. In this study, quaternary Cu-Al-Ni-Nb shape memory alloy was produced and for 1, 2, 3, 6, 12, and 24 hours it was kept at 1073K. The as-quenched and heat-treated alloys were investigated. The alloys were showed high-temperature shape memory characteristics and the aging increased its martensitic phase transformation temperatures. Additionally, the alloy lost its shape memory properties for 24 hours aged at 1073K. Furthermore, other thermodynamics parameters were affected through an increasing time of aging. It was found that 3 hours aged sample has minimum enthalpy change for martensite phase transformation. On the other hand, map analysis of the composition illustrated that copper and niobium did not dissolve to each other, nickel was homogeneously distributed, and a low concentration of aluminum dissolved in the Nb-rich phase compared to the matrix.

Keywords: High Temperature Shape Memory Alloy; Phase transformation; Cu-Al-Ni-Nb; Heat treatment; Thermal characteristics

ÖZET

Cu-Al-Ni-Nb DÖRTLÜ ŞEKİL HATIRLAMALI ALAŞIMLARIN FİZİKSEL ÖZELLİKLERİ ÜZERİNE ISIL İŞLEM ETKİSİNİN İNCELENMESİ

Bahar Ali Mohammed FARAJ
Yüksek lisans Tezi
FIRAT ÜNİVERSİTESİ
Fen Bilimleri Enstitüsü
Fizik Anabilim Dalı

Şubat 2020, Sayfa: viii + 45

Endüstri ve diğer alanlar çalışmalarında genel olarak kullanılan önemli uygulamalardan biri ısıl işlemdir. Yaşlandırma zaman ya da sıcaklığa bağlı olabilen bir çeşit ısıl işlemdir. Bu çalışmada, Bu çalışmada, dörtlü Cu-Al-Ni-Nb şekil hatırlamalı alaşım üretilmiş ve 1073 K de 1, 2, 3, 6, 12 ve 24 saat bekletilmiştir. Ani soğutulan ve ısıl işlem yapan alaşımlar incelenmiştir. Alaşımlar yüksek sıcaklık şekil hatırlama karakteristiği göstermiştir ve yaşlandırma alaşımın dönüşüm sıcaklığını arttırmıştır. Buna ek olarak, alaşım 1073 K de 24 saat yaşlandırma sonrasında şekil hatırlama özelliğini kaybetmiştir. Ayrıca, diğer termodinamik parametreler yaşlandırma zamanın artmasından etkilenmiştir.3saat yaşlandırılan numunenin martensit faz dönüşümü için minimum entalpiye sahip olduğu bulunmuştur. Diğer taraftan, Diğer taraftan kompozisyonun haritalama analizi; bakır ve Niobium alaşım içinde çözülmemiş, nikel homojen olarak dağılmıştır ve düşük konsantrasyonda alüminyum elementi Nb zengin faz ile kıyaslanırsa, matriks içinde çözülmüştür.

Anahtar Kelimeler: Yüksek sıcaklık **ş**ekil hatırlamalı alaşım;faz dönüşümü; Cu-Al-Ni-Nb; ısıl işlem; termal özellikler

LIST OF FIGURES

Page no.

LIST OF TABLES

Page no.

List of Symbols and Abbreviations

Symbols

A_s	Austenite start temperature
A_p	Austenite peak temperature
A_f	Austenite finish temperature
M_s	Martensite start temperature
M_p	Martensite peak temperature
M_f	Martensite finish temperature
σ_s	Starting stress
σ_f	Final stress

Abbreviations

A	Austenite
M	Martensite
SMA	Shape Memory Alloy
Cu	Copper
Al	Aluminum
Ni	Nickel
Nb	Niobium
Fe	Iron
Zn	Zink
SME	Shape Memory Effect
PTT	Phase Transformation Temperature
HTSMA	High Temperature Shape Memory Alloy
SIM	Stress-Induced-Martensite
ASTM	American society for testing and materials
DSC	Differential Scanning Calorimetry
SEM	Scanning Electron Microscope
EDX	Energy Dispersive X-ray spectroscopy
XRD	X-Ray Diffraction

1. INTRODUCTION

In ancient times materials have significant factor to develop a history of human life. In the different periods of time material has an important role, such as the Stone Age, Bronze Age, Iron Age and renaissance. With developing technology and science, and a better understanding of the material's behavior, material science have been got more attention in various field of studies and application [1]. In addition, by changing thermal, electrical, magnetic and/or mechanical characterization of materials, the materials are made a wide range of applications [2-4].

Nowadays, shape memory materials are one of the most commercial that able to memorize their shape and when they deformed, they can return back to pre-determined shape by only heating to a particular temperature. Due to superelasticity and strain recovery, SMAs are used in the industrial [5, 6], automotive [7, 8], the thermal actuator [9], aerospace [10, 11], engineering, and biomedical application [12-14].

SMAs exhibit two-phase, which are austenite phase (parent phase) and martensite phase called product phase. The product phase can be in either twined or detwinned [15]. The most commercial alloys of shape memory materials are NiTi-based alloy [16], copper base alloy [17-19] and Fe base alloy [20]. NiTi alloys are most commercial ones, but they are intricacy and having expensive costs comparable with copper-based alloys, so copper-based alloys are sometimes used instead of NiTi alloys in lots of application. Cu-based SMAs have excellent functionalities and they easily can be manufactured, which enhanced their applications [21]. Moreover, they have various types with different compositions and additional elements such as Cu-Zn, Cu-Al, CuAlNi, CuAlNb, and CuAlBe. Among the aforementioned Cu-based alloys, CuAlNi is the most widely used because this ternary system of the alloy has good thermal stability, great recoverable strain, high transformation temperature and good thermal and electrical conductivity [22].

In chapter two of this study, SMA has defined and an important invention and investigations were mentioned briefly. In addition, the specific properties of SMAs were explained. Then three copper-based shape memory alloy has overviewed using some related diagrams. Furthermore, CuAlNi alloy has clarified. In the third chapter, the methodology and the materials in use has been explained. The fourth chapter deals with the results in term of tables and graphs, also the obtained result in either experimental or calculated ones has been discussed and supported by literature. Lastly the conclusion and main outcomes of this study briefly given in chapter five.

2. SHAPE MEMORY ALLOY

SMA can be defined as a group of materials in the shape of alloys that display shape memory properties and have the ability to recover to pre-determined shape after changed shape by upload heating or loading on it. Even the alloy under high applied load due to increase temperature the shape can recover. Under specific terms, in addition, when SMAs subjected to applied mechanical load SMAs can dissipate and absorb mechanical energy by undergoing a reversible hysteric shape change. SMAs have been widespread due to the unique characteristics especially for impact absorption, vibration damping, and actuation and sensing applications. However, SMAs display low-frequency response but there is a group of materials called magnetic shape memory alloy which has lately been investigated achievable higher actuation frequencies. Also the performance of SMAs always expansion in a wide different field of industrial application like biomedical, oil utilization, automotive and aerospace. Also in the last decades, many works of SMAs have explored the application of SMAs, engineering effects and microstructural mechanisms, including the comprehensive summaries of Perkins, Funakubo, and Otsuka and Wayman [23], the experimental action of Jackson [17] and colligates and the application considerations of Duerig [24] and other.

2.1. A Brief History

In the 1890s, Adolf Martens took the foremost step in the discovery of the martensite in the steel. The transformation of martensitic is a metallic phenomenon that was probably studied in the early 1900s on a large scale. The martensitic Shift As noted in the Fe-c system, this transformation was established as an irreversible process. In 1949, by Krodomov [25] and Candros, the martensite transformation of thermocouple showed the reverse transformation of Martensite, based on the experimental observations of the thermal reflective structure of the CuZn and CuAl spiders. In other spikes such as InTI and CuZn, the thermoplastic martensitic was confirmed in 1953. The reflective conversion and the alloys exhibited above were not used until 1963. But after the discovery of NiTi a breakthrough event for engineering applications this was discovered by Buhler [26] and his colleagues working during the investigation of useful substances to protect from heat. It is noted that NiTi has good mechanical properties and its ability to recover its shape, so it can be compared with some common engineering metals. NiTi has been formulated for NiTiNOL in recognition of its discovery at the Naval Ordnance Laboratory (NOL). Its composition and the effect of heat treatment and its structure were examined on a large scale. Other studies [27] showed in 1965, with the addition of the third alloy component to the NiTi system such as Co or F made a decrease in the transformation temperature of SMA. When Cryofit that new alloy of SMA used as a first commercial application in F-14 aircraft for pipe coupling [28]. In 1989 due to continued research for the development of SMA, led NiTiNb system produced and used in many application of battle damage [29] repairs and also used for repairs in nuclear reactors because this alloy had big temperature hysteresis and easy to handle. In 1970 [30] were developed HTSMAs mean high-temperature shape memory alloys that transformation temperature of these alloys more than 100 C, these alloys such as TiPd, TiPt and TiAu. By continued studying on the properties of NiTi alloy In 1978 [31]by Meanwhile, Melton and Mercier showed that the alloy of Cu with material tight the hysteresis stress and there were not change considerably transformation temperature. Also, Miyazaki changed the life of alloys in 1999 due to improvement in NiTiCu alloys [32], which these changed made used these alloys in the many engineering application due to low cast and improve fatigue life.

Much commercial application have been developed since the initial discovery in 1963 of nitinol, some application in the field biomedical of NiTi appeared during 1970, in 1990 NiTi alloys made their commercial penetration and in this time NiTi used in many application of electronic cable connectors, air conditioning vents, valves and an assortment of other products. In addition, in the field of oil industries and aerospace ordered over the last decade for actuation under high-temperature operation conditions, it also revived a massive deal in the development of HTSMAs. Lastly, some alloys under investigation but different, because these alloys display shape change characteristics such as SMA but under the impact of a magnetic field [33, 34].

2.2. Phase Transformation in Shape Memory Alloys

In the schematic of materials for the metallic alloy, a metallurgical phase diagram represent equilibrium condition. Due to phase boundaries or equilibrium lines that consisted of phase diagram separate dissimilar phases from each other. For producing any alloy have to consist of two or more elements, generally, temperature variable used along the y-axis and the concentration represented along the x-axis that becomes an important variable. Also, there are some other control variables in the phase diagram that used and represented along both axes of which the equilibrium phases such as (temperature, electric field, stress, concentration etc.). The disassociation and formation of phases are shown with the change in temperature, at fixed composition for an alloy. In a similar way, SMAs with typical operating temperature range has two phases both of these phases with a various properties and various crystal structure, those are austenite (A) in high-temperature phase that generally cubic with different crystal structure with compare to another phase, and the second is martensite (M) in low-temperature phase and in (monoclinic, tetragonal or orthorhombic). By sheer lattice, distortion occurs transformation from one structure to the other and does not transform by diffusion of atoms. This transformation occurred called martensite when the alloy transformed from austenite phase to martensite phase, for each martensitic have various orientation direction in crystal formed and called variant, and the assembly of variants in martensitic can occur in two forms those are twinned martensite and detwinned martensite which formed by a combination of self-accommodate and specific variants respectively. Also, austenite referred to as the parent phase and martensite referred to as the product phase, which forms the basic behavior of SMAs due to the reversible transformation from these two phases from austenite to martensite and vice versa.

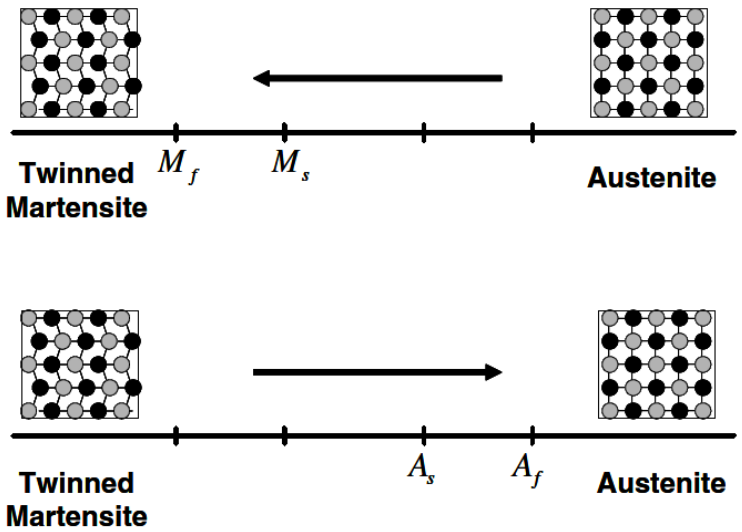

Figure 2.1. Phase transformation temperature from austenite to martensite and vice versa [35].

When crystal structure in the parent phase and upon cooling without applying load changes from the parent phase to product phase, and this transition named forward transformation. After transformation, there are several crystal orientation directions occur (variants) for NiTi up to 24. The arrangement of variants happen to result in twinned martensite and the average macroscopic change is insignificant. Also, reverse transformation occurs when crystal structure in the product phase and by heating without loading and which there is no associated shape change during this process, the alloy return back to the parent phase. Figure 2.1 shows the phase transformation between martensite to austenite and vice versa with the corresponding schematic crystal structure.

In the phase transformation, there are 4 characteristics of temperatures associated. In the forward transformation, there is austenite, in the absence load, martensitic start temperature (M_s) that is when the phase starts to transform to twined martensite and martensite finish temperature (M_f) that is when completing the transformation to martensite, in this case, the material is fully in the twined martensitic phase. In a similar way, when the material heated the phase transformation happens to return back to the austenite phase, at the start of transformation the material in austenitic start temperature (A_s) and when the transformation completed is in the austenitic finish temperature (A_f). But when the material in the twined martensite if mechanical load loaded on it especially in low temperature, it's possible to transform material to detwinned martensite by reorientation of specific numbers of variants as shown in Figure 2.2. This process happens by macroscopic shape change, where the deformed arrangement must keep after unloading.

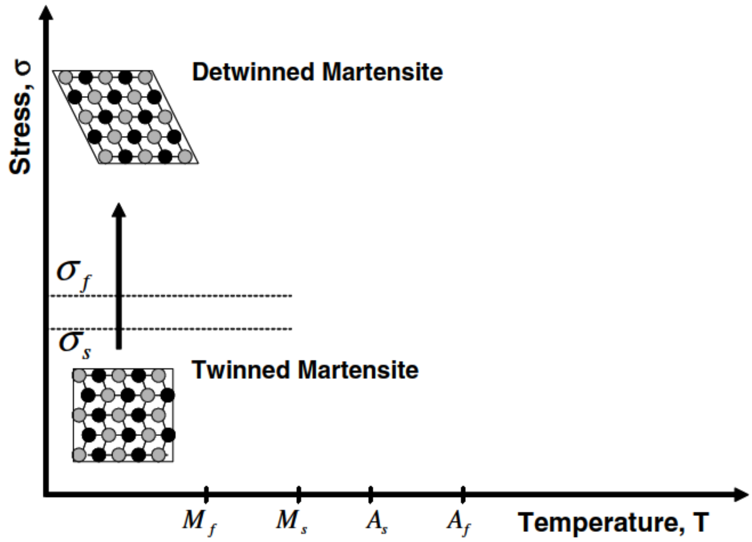

Figure 2.2. Twinned martensite to detwinning the martensite phase by applying stress [35].

Shape recovery completed if the SMA heating to a temperature that more than austenite finish temperature, in that time it will be result transformation from detwinned martensite to austenite and this is a reverse transformation in Figure 2.3. It also shows that and if material getting down temperature to under martensite finish temperature the material with no associated shape change return back to twined martensite and this is forward transformation. This process that talked is one property of SMA, which is shape memory effect (SME).

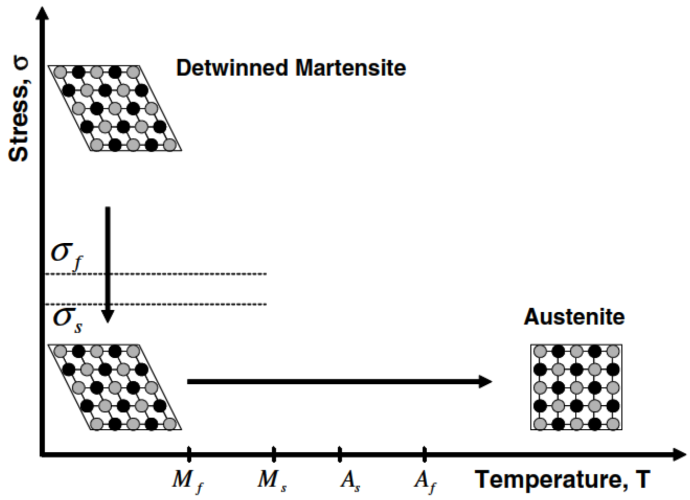

Figure 2.3. Reverse transformation between detwinned martensite and austenite phase by heating [35].

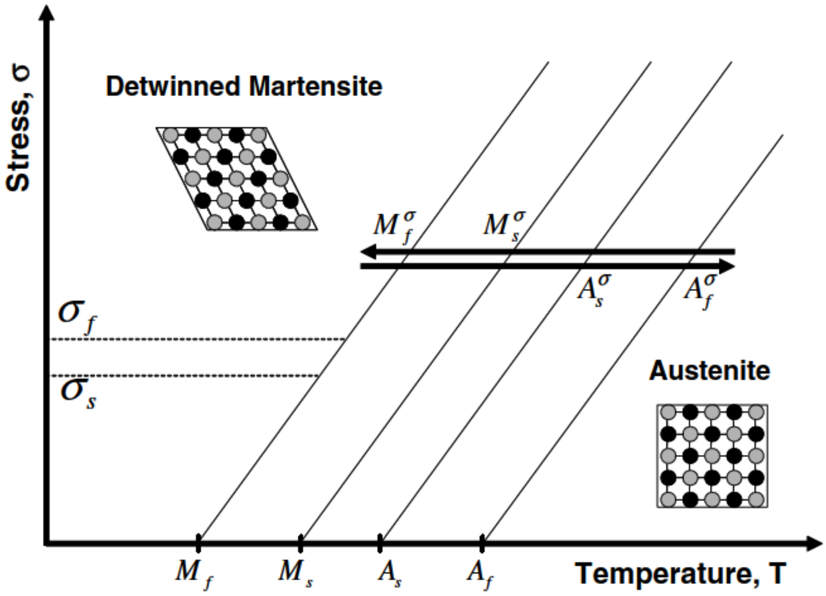

Figure 2.4. In the existence of load, phase transformation for stress-temperature [35].

For making the detwinned process, it must the load that applied to the material enough big to start the process. The detwinning start stress (σ_S) is the minimum stress that needed to make start to detwinning process and the finish stress detwinning (σ_f) is the result of the complete detwinning process that occurs after sufficiently high load on material. When mechanical load that more than detwinning start stress applied on the material in the austenite phase and the material cooled, produced a shape change in the material because the phase transformation will result forming detwinned martensite, also without any change in the applying load when reheating the material shape recovery happen (Figure 2.4).

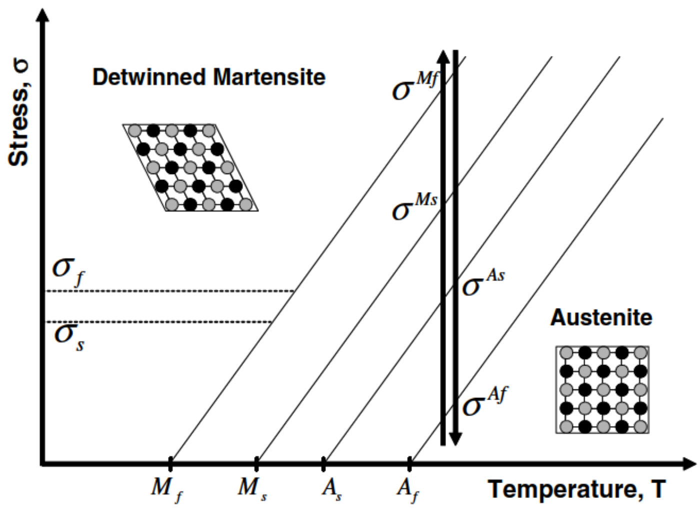

Figure 2.5. Loading and unloading path of superelasticity [35].

Recognizing that both cases of transformation reverse and forward, are happening in the domain of (A_s to A_f, M_s to M_f) respectively for a composition of given shape memory alloy, we can build the area of transformation in the stress-temperature space. There is a strong relation between transformation temperature and applying load because when the magnitude of applied load is high, the transformation temperature leading in high, which is mean with increasing magnitude of applying load increasing in the transformation temperature. In stress-temperature space, the transformation A→M_d and M_d →A have a positive slope The new transformation temperature with corresponding stress (σ) under applied uniaxial load is represented as (austenite start A^s_σ, austenite finish A^f_σ, martensite start $M^s\sigma$ and martensite finish M^f_σ) temperature and σ referred to magnitude of stress. In addition, the other properties of SMA is pseudoelastic PE or superelasticity SE, that thermally induced transformation occurred when sufficiently mechanical load applying on the material in the austenite phase and the result be fully detwinned material but not stable phase and when unloading on the material if the temperature of the material more than austenite finish temperature, then shape recovery happen and material return back to the austenite phase. Figure 2.5 shows the loading and unloading path of PE, and in Figure 2.6 represents a stress-strain diagram that captured macroscopic shape change by the applied load.

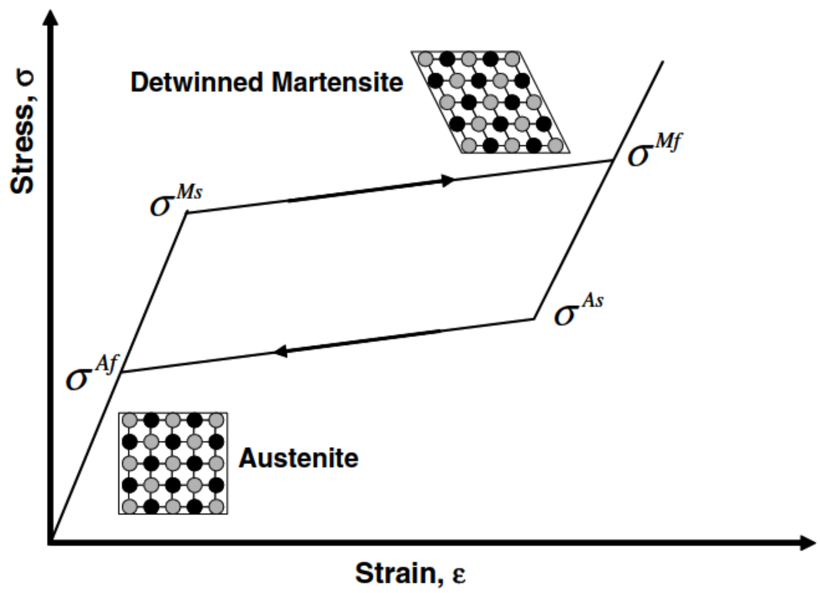

Figure 2.6. The stress-strain diagram for superelasticity [35].

σ^{Ms} is denoted starting martensite transformation at which in the stress level and σ^{Mf} is completing transformation temperature at which in the stress level. In a similar way, when unloaded on the material, the stress level at which the transformation reversed to austenite in the starting of transformation denoted by σ^{As} and in the completing of transformation denoted by σ^{Af}. Only partial shape recovery observed if the material in the austenite phase and tested the phase between austenite finish temperature and martensite start temperature. In the Figure 2.7 in stress-temperature diagram showed various phase of shape memory alloy that include each twined and detwinned martensite and austenite phase with the region of transition, and by this diagram that clarifies various diagram in stress-temperature and fixed composition of SMA, materials are called phase diagram, the base of construct this diagram include the shape memory alloy material response subjected to different thermo-mechanical loading paths resulting pseudoelastic and shape memory actuation behavior.

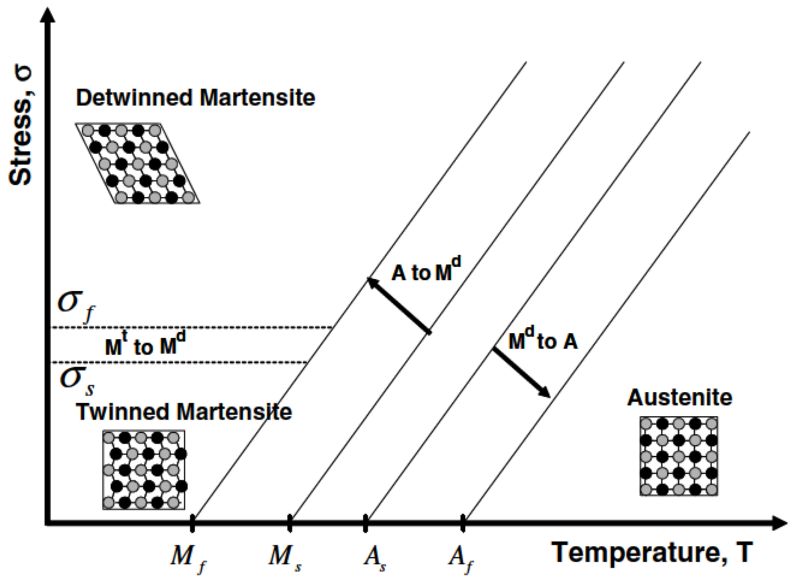

Figure 2.7. The stress-temperature diagram showed the various phase of shape memory alloy [35].

In the two following sections discussed both shape memory effect and pseudoelastic behavior of shape memory alloy in detail.

2.3. Shape Memory Effect

The important property of SMAs is shape memory effect when it is deformed in twined martensitic and unloaded while at a temperature under austenite start temperature when it is heated subsequently to more than austenite finish temperature than the material recovered shape and return back to parent phase. In the Figure 2.8 in the stress-strain-temperature diagram that resulted from experimental data for a NiTi sample that tested under uniaxial load explaining shape memory effect for better understood in this property that following thermo-mechanical load path, through applied load on the sample stress σ is uniaxial and strain ε is the change in the length along the direction of the load that applied on the sample.

In the beginning in Figure 2.8 in point A in austenite phase, by cooling the sample in stress-free in point B under martensite start and finish temperature (below forward transformation temperature), twinned martensite was formed (in point B).

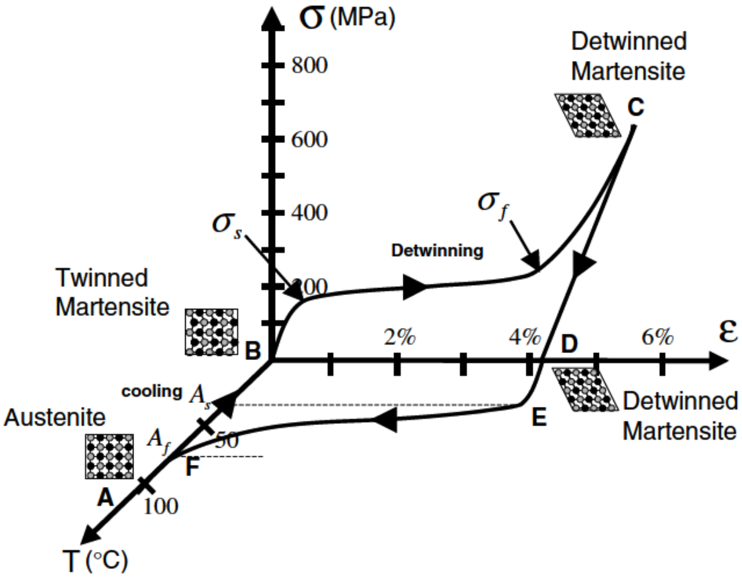

Figure 2.8. A NiTi sample experimental stress-strain-temperature data that display SME [35].

By applying stress on the sample when in twined martensite that this stress has to more than the start stress level (σ_s), the process of reorientation started and making the development of a specific oriented martensite variant. The stress level is far lower than the lasting plastic yield stress of martensite for the reorientation of the variant. In the point C, the process of detwinning martensite is completed in the stress level σ_f that at the end of a plateau characterized that showed in Figure 2.8 in the stress-strain diagram, and then the material elastically from point C to Point D unloaded and keep the detwinned martensite state. Without of stress by heating the sample to the temperature of austenite start temperature, the reverse transformation starting in the point E and in the point F the transformation completed at austenite finish temperature, also in the upper of this point the parent phase has occurred. Without existing of lasting plastic strain produced detwinning martensite and retained the original shape of the sample in point A. Although by changing phase transformation in the detwinned martensite to austenite produced a strain recovery and termed transformation strain and denoted as (ε_t). Also by getting down the temperature of the material to martensite generated again self-accommodate twinned martensite variant and there was no changing in the shape and can repeat the entire cycle of the shape memory effect, by this phenomenon of shape memory effect called simply or one-way shape memory effect. Because in this phenomenon the material has been detwinned when the mechanical load applied on it and then heated the material then shape recovery achieved. For more explanation of SME in the example, 1.1 consider an example of shape memory alloy's specimen such as a wire used in this example that the diagram showed in Figure 2.8 in stress-strain-temperature, this wire used for the application actuation for one time. When the wire in the twined martensite and under the temperature of martensite finish, when applied load on it and stretched along axial direction, due to elastic behavior of the wire try to display this behavior until specific stress elastically deformed but when the stress due to the loading reaches about 150MPa the wire start to elongated with a bit increase in the stress level, and this point as starting detwinned martensite determined. The process of detwinning be continuous until the whole of the wire detwinned and in this point total strain about 4%. At this point, the wire starts to become stiff with an increase of stress. In the diagram the finishing process of detwinned is determined in the end of the slop over loading. When the stress released on the wire, then the wire detwinned unloads elastically and through the detwinning the strain induced not recovered. This detwinning used in actuation application. Through the process of this application using a thermal source for heated wire like resistive heating, with increase of temperature the wire start to expansion, and when temperature reaches about room temperature (austenite start temperature) the process of detwinning changes to transform to austenite. Also this result in contraction of shape memory alloy and when increasing temperature more than 70 the actuation process is finished and the wire reaching state of austenite. The entire A_f will rely on stress of shape memory alloy through reverse transformation.

2.4. Pseudoelasticity

The pseudoelastic or superelasticity is the second property of shape-memory materials, this behavior is associated with stress-induced transformation while leads to produce strain through applying load and after onto unloading strain recovery at a temperature that more than austenite finish temperature. In general, the path of thermo-mechanical loading in pseudoelastic begins in the austenite stable phase at enough high temperature and by an applied load on the material the phase transform to detwinned martensite stable phase, lastly, this phase returns back to the parent phase when the stress realized and no stress on the material.

Figure 2.9 shows an example of the pseudoelastic loading path (a → b → c → d → e → a). Generally for applying the test of pseudoelastic constant temperature that more than austenite finish temperature performed. Also, path two that showed in Figure 2.9 is a test of loading path, and for more explanation of understanding pseudoelastic behavior in detail, consider path two (A → B → C → D → E → F → A) is thermo-mechanical loading path. Which beginning at a temperature more than austenite finish temperature and zero stress. In point, A → B showed that when the mechanical load on the material applied and material in the austenite phase then the material undergoes elastic load. On a certain level of the load, the path of the load intersects with the surface for beginning martensite transformation in the phase diagram, and this point noted as the stress level (σ^{Ms}) that making occur starting martensite transformation. Note that due to the transformation by stress-induced from austenite to martensite that accompanied by the production of huge inelastic strain that showed in the diagram of Figure 2.10 for diagram of stress-strain experimental data loading path.

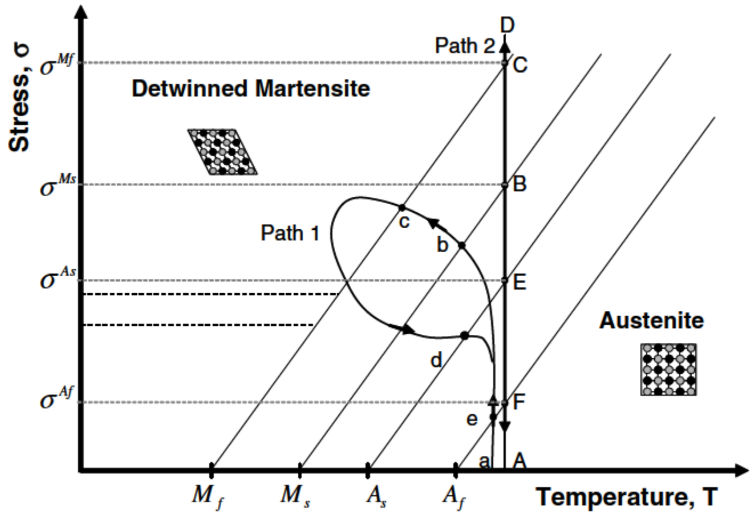

Figure 2.9. The stress-temperature phase diagram loading path of pseudoelastic [35].

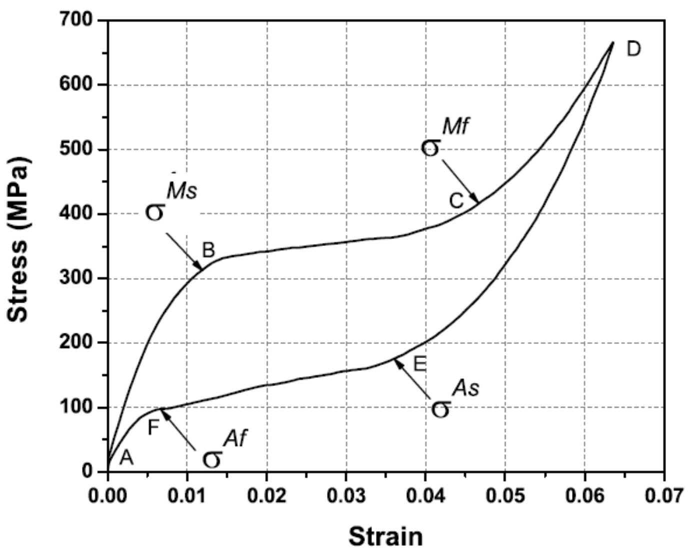

Figure 2.10. The stress-strain diagram loading path of pseudoelastic behavior [35].

In point (B → C) the transformation proceeds to the stress level (σ^{Mf}), intersected transformation of martensite finish temperature by the loading path and this is marked as the finish of transformation. A distinguished change determined in the slope of the stress-strain curve as the finishing process of martensite transformation that associated with elastic loading of the phase. After increasing the magnitude of stress on the material, the elastic deformation of detwinning martensite exist and there is no transformation as shown in point (C → D). Also when unloading the stress on the material the martensite phase elastically unloads as shown in the point (D → E). At σ^{As} the austenite start intersected by unloading path at point E, and this reason makes the material return back from martensite to parent phase. This process is accompanied by the recovery of strainthrough the transformation of phase in the finishing of unloading. In the point of re-joins, the elastic area of austenite in the curve of stress-strain loading denoted as the finish transformation back to austenite, in the point F corresponding to stress austenite finish temperature. Then elastically the material unloads to point A. Through complete the cycle of pseudoelastic, the forward and reverse transformation of phase consequences in a hysteresis, which represents the energy dissipated in the space of stress-strain in the cycle of transformation. The size of hysteresis and stress level transformation relies on the test conditions and type of the shape memory alloy material. The path of 1 or 2 in Figure 2.9 is path of applied stress on the material and result made detwinned martensite from austenite phase and this form is one of the stress-induced-martensite (SIM) form, this form can be formed by many thermo-mechanical loading paths, generally, SIM is forming martensite phase from austenite by applying stress on material.

In general, pseudoelasticity is used as terming that have two behavior those are rubber-like and superelastic [36]. Superelastic is the behavior that occurred when by thermo-mechanical loading path on material caused a reversible transformation phase that described in the above paragraph, and the behavior of rubber-like is so exclusive to exist because only by reversible reorientation of martensite occurred. Some times in the elderly process of martensitic phase at temperature under martensite finish temperature and in the process of unloading can enable reversal detwinning martensite, which the resulting is similar to the result of the stress-strain curve of superelastic and this event is called rubber-like effect that similar to elastic of nonlinear behavior of rubber. But the stress that needed to detwinned martensite in rubber-like is tiny with compare to the stress level that makes starting martensite transformation. Therefore, does not consider rubber-like effect moreover and considered pseudoelasticity only refers to superelastic.

2.5. Behavior and Characterization of SMA

For attaining the quantitative properties and behavior of indication qualitative of shape memory alloy material can attain from the characterization of thermomechanical (Figure 2.11). Differential scanning calorimetry (DSC) was used to determining behavior and property of the material in four various conditions, resolving transformation in zero σ, loading monoclinic and unloading monoclinic, in the above of zero stress level resolving shape memory effect, in the final effect of again doing loading when the material in the equilibrium. Consider in actuator application used a wire 0.91 mm in diameter of NiTi, it`s needful to learning the free transformation temperature of stress So as to determine the transformation of zero stress, on the other hand determining phase of the alloy is very complicated in any liable of temperature and stress. Additionally, Figure 2.12 shows the result of loading and unloading of the monotonic test.

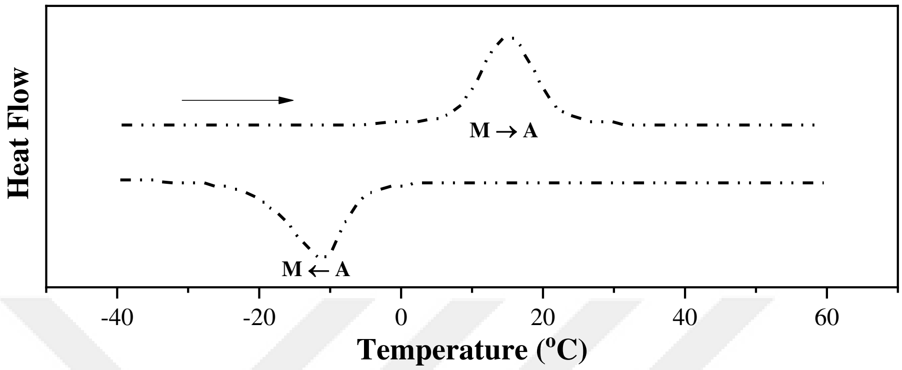

Figure 2.11 Result of a DSC measurment [37].

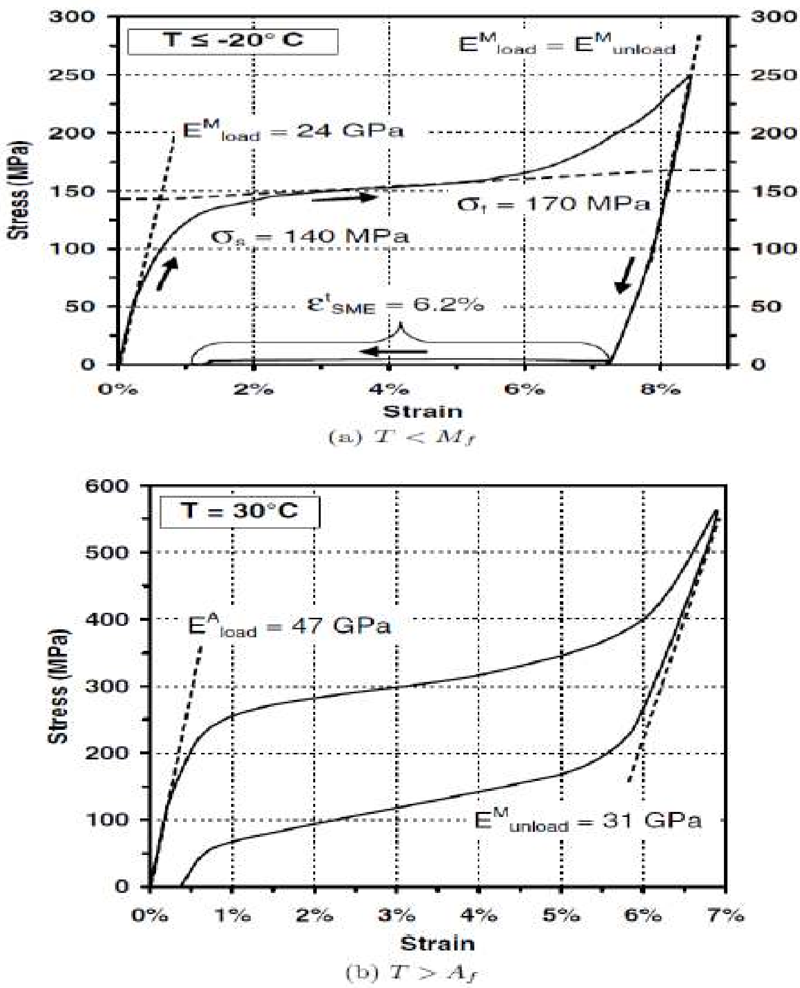

Figure 2.12. Result of loading and unloading of the monotonic test [37].

A device of differential scanning calorimetry is used so as to determining these temperatures. For measurement material in DSC, cut the material into small piece and put in the DSC for a time and waited until the heat flow/temperature showed tangent to each peak of start and finish and curves showed on the screen of the DSC computer, and heat will flows if drawn a tangent to baseline. The beginning and finish temperature of every transformation measured by the various intersection of these lines.

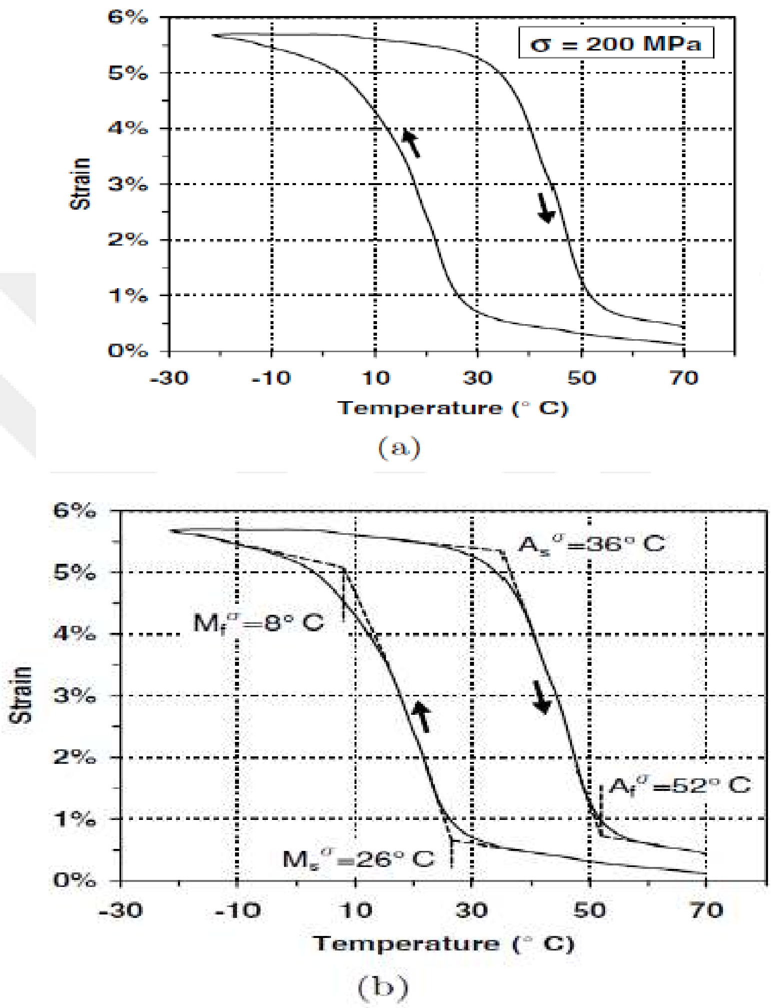

Figure 2.13. Under constant stress thermal cycling a) curve of temperature strain loading and b) transformation temperature [37].

In Figure 2.13 shows a under constant stress thermal cycling, curve of temperature strain loading and transformation temperature. Consider SMA tested by monotonic loading if martensite finish temperature bigger than temperature (i.e. T<-20 ºC) if the material shows the important behavior of shape memory by attaining the potential to expression stress-free shape memory effect, gives lightening and identify on elastic properties of twinned martensite. Prior testing, the specimen at start is heated up to more than austenite finish temperature (i.e. 22 ºC) to recovery any strain transformation and after got down temperature to under martensite finish temperature (i.e. -20 ºC) to gain martensite state fully, and due to this formation of unknown detwinned martensite does not occurred that by unknown deformation formed. As a result, the fragment tested at a temperature under martensite finish temperature, and the only phase of the balanced phase is martensite. When detwinning had completed, extreme stress is chosen through the course of testing. Then the sample unloaded and homogeneously increased the temperature of the sample up to austenite finish temperature, and any recoverable strain existed is examined. In this test detwinned start stress (σ_s) is 140Mpa and detwinned finish stress (σ_f) is 170MPa and strain recovery approximately 6.2% and the other non-recoverable stay to the finished test of shape memory effect, obtain 24GPa for elastic modulus. If the temperature about 30C which means more than martensite finish temperature, the monotonic loading applied to the sample then obtained complete super elasticity property with Continuous plastic strain. In this case that temperature more than martensite finish temperature compare to previous cases that temperature smaller than martensite finish temperature, the martensite elastic modulus is higher in this case, and ma remains some part of austenite for after finish of loading. According to American society for testing and materials (ASTM) test method F-2516 elastic modulus through unloading will reflect martensite and austenite. In the time of loading at strain 300MPa and stress 3% in the upper level and at strain 100MPa stress at 2.5% in the lower level, 47GPa has founded for elastic modulus.

An actuator in the time of more than zero stress must examine zero shape memory effect and material is able to complete the work by providing dislocation under the load. Isobaric test is the test that stress actuation is constant will be adopted for uniaxial loading, for instance, a specimen of shape memory alloy is increasing temperature to more than austenite finish temperature (i.e. 22ºC) and after applied stress to 200MPa and this load remaining constantly, when temperature slowly deceased until finished forward transformation into martensite, after increasing temperature by mildly until completed reverse transformation. The strain registered and examined over this experiment.

In the time of cyclic loading, when shape memory alloy deals with numerous transformation cycles a strait forward oncoming occurs of execution abundant cycles of thermal transformation able to applied below fixed load. For reversal and repeated loading, about 200Mpa or under this magnitude in constant is performed. Comprehensively adopted about eighty thermal cycles. The material response has stabilized and appeared when subjected to cycling load. The range of the stresses from 2 to 200MPa in 50Mpa accession, for determining transformation stress and transformation temperature in zero stress, test of low stress is important.

In Figure 2.14a display spectra EDX of the NiTi shape memory alloy which displays NiTi and $NiTi_2$ phase circulates in the matrix phase of the NiTi shape memory alloy and due to existing of $NiTi_2$ in the matrix, the matrix rich in Titanium. Also, the DSC curve shows in Figure 14b due to the existing $NiTi_2$ phase, the transformation temperature decreased in the NiTi shape memory alloy through melting and solidification, by lowering transformation temperature nickel increased concentration of the matrix. The result of XRD analysis showed in Figure 2.14c that in the NiTi shape memory alloy consist of Austenite phase B2 and martensite phase B19′ and phase of $NiTi_2$ at the same time which this is an agreement with the test of DSC. Austenite and martensite exist at the same time, which is due to that the martensite finish temperature of NiTi shape memory alloy is lesser than room temperature and this causes insufficient transformation at room temperature from austenite to martensite of the NiTi shape memory alloy.

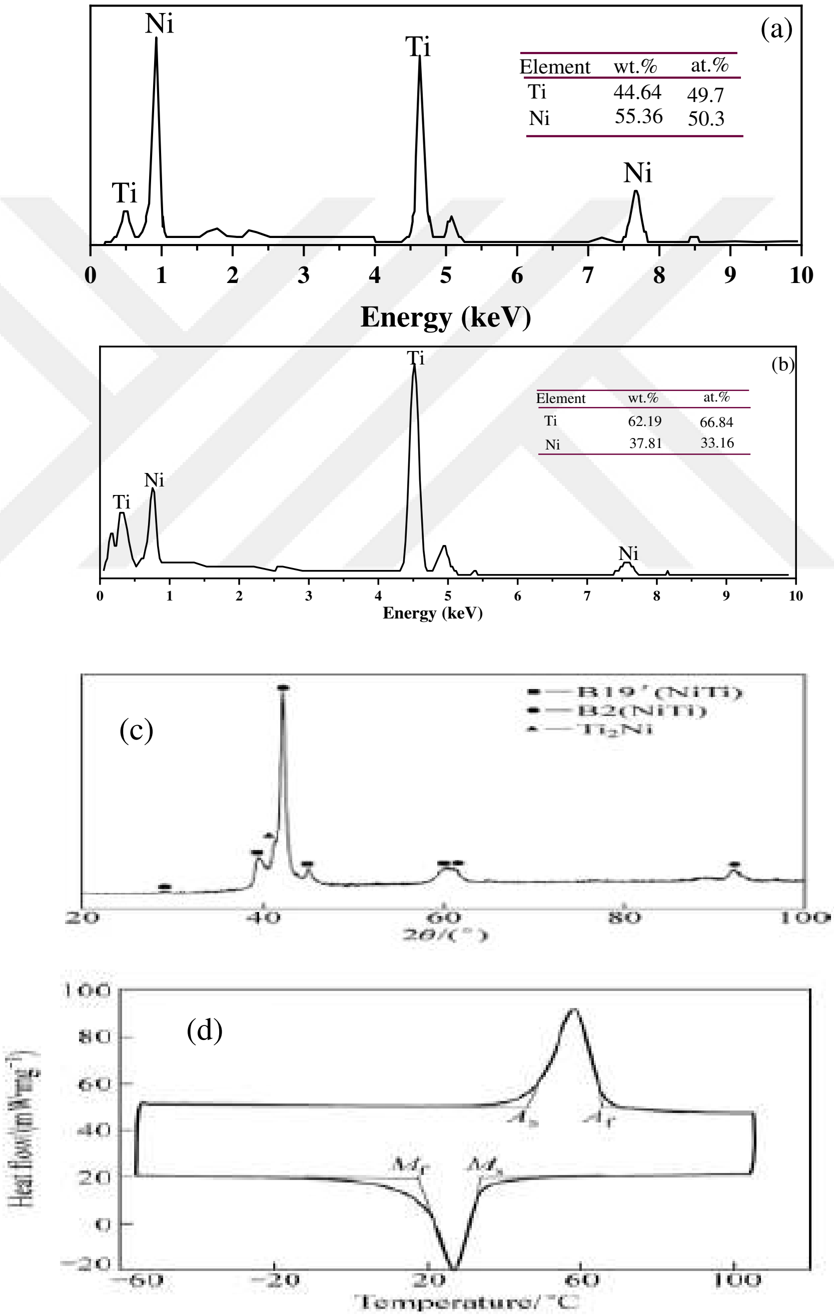

Figure 2.14. The result of (a and b) EDX spectra testing, (c) result of XRD testing, and (d) result of DSC testing [38].

2.6. Cu-Based Shape Memory Alloy

SMAs have some types of alloys between them NiTi alloy is good alloy and display a good biocompatible and both propertied behavior of pseudoelasticity and shape memory effect, but NiTi alloy expensive with compare to Cu based alloys and the properties that make alternating Cu-based alloy using instead of NiTi alloy is that Cu based have good thermal conductivity and electrical. In general Cu based alloy display hysteresis that less than from NiTi alloy, and in the copper-based alloy transformation temperature extremely reliant on the composition of the alloy. Some times to attain reproducible transformation temperatures it is needful to change accurate 0.001 to 0.0001 atomic percentage within the extent of 5◦C. Cu-Al and Cu-Zn are found as the main base alloys of Cu-based, in this section will discuss extreme commonly copper-based alloys that used to shape memory alloys materials. The binary of Copper-Zinc alloys is one of the most commercially used types because these types have resistance to intergranular fracture and very ductile as compared with other alloys of copper-based [33].

Also in the temperature under 27 ◦C these alloys transforming to the state of martensitic. In addition, the third element to the copper-zinc alloy can change in the transformation temperature such as aluminum can increase in the transformation temperature when added to Cu-Zn binary alloy. Also, changes in the ratio of aluminum in the composition from 5 to 10 weight percentage can changing in the martensite start temperature, shifting from about -90K to 370K. Although when the alloy becomes very hot or old in age, the austenite phase displays a strong tendency toward decomposing into its equilibrium phases, and due to this reason usually the operating temperature limited to about 370K. The transformation temperature is very sensitive to the composition of the alloy and in the operating process of melting can be lost so for sake of this reason the fabrication process must to exactly controlled.

Also, CuAlZn alloys are extremely sensitive to heat treatment like that in the transformation temperatures the quenching rate can lead to phase changing or dissociation. Also due to that these alloys have low critical stress for sliding their mechanical behavior and are restricted to levels of stress about $2*10^8$ Pa. These alloys display excellent superelasticity and shape memory effect in the operation of extent stress, but the transformation of the strain is restricted to approximately three to four percentage [33].

Copper-Aluminum-nickel (CuAlNi) [39] is also one of the most useful of copper-based alloys and fewer sensitive as compared to the previous alloy in the phenomena of aging and stabilization. The next section will more be explaining. In the last few years ago there are some other alloys that have studied and developed such as CuAlBe, CuAlMn that has good ductility and CuAlNb that has appropriate for application in high temperature.

2.6.1. Phase diagrams of typical Cu-based shape memory alloys

Although NiTi alloy display good behavior in ductility, corrosion resistance and strength which are very useful for using in practical but this materials are expensive so in addition to instead NiTi alloy due to expensive of materials Copper-based alloy advanced and investigate, which have useful in deformability and good thermal and electrical conductivity, copper-zinc and copper-aluminum alloy have investigated in the family of copper-based alloy.

The transformation temperature martensite start of the high-temperature disordered phase, body-centered cubic structure (β) phase copper-zinc binary in about 40 at% zinc is distant under room temperature, and when zinc in the content alloy lesser than approximately 38at% a great transformation exist, which is diffusional phase change but is composition invariant. Some materials like Sn, Si, Ga and Al are added to the copper-zinc alloy for stabilized β phase and increasing martensite start transformation. Belong them, the ternary of copper-zinc-aluminum shape memory alloy are the greatest excellent with respect to grain boundary fracture and ductility.

Figure 2.15 shows the vertical section of a phase diagram in equilibrium for the content of aluminum of 6mass% in the composition of ternary Cu-Zn-Al. In here, β phase is the high-temperature phase is disordered body center cubic, but onto quenching to ambient temperature ordering exist to B2 (CsCl type order structure) or $D0_3$ (Cu_3Al type ordered structure) and then this phase transforms to 9R (rhombohedral period9) or monoclinic martensite structure 18R (6M) without or with cooling, relying on composition of alloy.

When increasing the ratio of aluminum, the phase of β is susceptible to decomposition to the face center cubic α (primary solid solution of copper) and cubic phase γ (Copper, Zinc) at about 425 °C. In the binary of Cu-Al system alloy the β phase undergoes a eutectoid decomposition into α and γ_2 cubic phase (Cu_9Al_4) at about 560C, but if quenched it from the area of β phase to ambient temperature, martensically transformed. The phases of martensite for lower than 11 mass% of Al are disordered 6M or 9R, for 11-13 mass% 18R (monoclinic martensite structure) and 2H (orthorhombic martensite structure) for more than 13 mass% of Al.

The martensite transformation before takes place the phase of β will be ordered for more than 11 mass% of Al. Even for the 14 mass% of Al the martensite start transformation is still over room temperature, and susceptible to Deposition of γ_2 for the alloy of upper content of Al and does not undergo the transformation of martensite. The precipitation of γ_2 suppressed when the third element of Nickel added to the alloy that is due to the diffusion of Al and Cu is discourage by adding nickel. In the alloy of content near 14mass % of Al and different content of Ni observed superb shape memory effect. Although with increasing Ni content to the alloy, the alloy will be brittle. Approximately Cu-14~14.5-Al 3~4.5Ni wt.%.

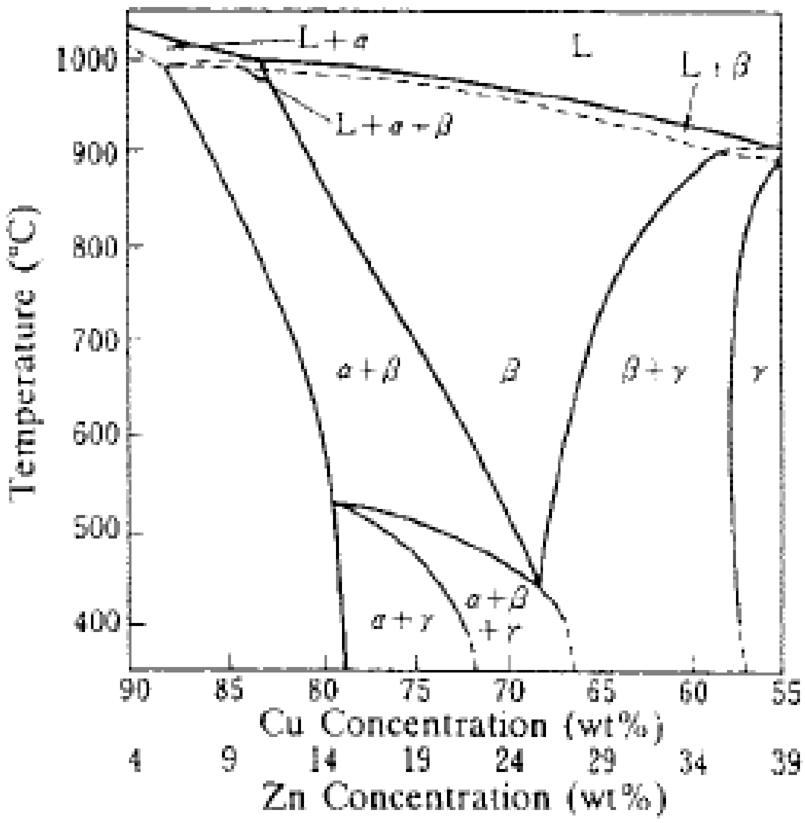

Figure 2.15. A ternary shape memory alloy of Cu-Zn-Al, the vertical cross-section of 6mass% of Al and phase diagram of alloy [20].

A vertical section of the equilibrium phase diagram in Figure 2.16 showes for the ternary alloy of Cu-Al-Ni at Ni 3 wt. %. NiAl in the Figure 2.16 as a product of the decomposition β is an equilibrium phase of B2. Fundamentally the martensite formed in the ternary shape memory alloy is similar to that in binary alloys relying on aluminum content. Additionally, Figure 2.17 shows the martensite start temperature as a function of composition for Cu-Zn-Al ternary alloys

Thus it is possible to adjust martensite start temperature of shape memory alloys by varying composition nearly between -100~200 C. As a function of x in Figure 2.18 displayed the martensite and austenite transformation temperature of Cu-xAl-4Ni mass%.

The Figure 2.18 can understand that with an increasingly small amount of x decreasing transformation temperature sharply. Although when Al amount is steady and by the increasing amount of Ni decreasing transformation temperature, the reliance of martensite start temperature upon Al is much stronger than that of Ni, and decrease M_s with an increase in the amount of Ni is effectively through increasing in the amount of Al. Although it must note that the main effect that used for

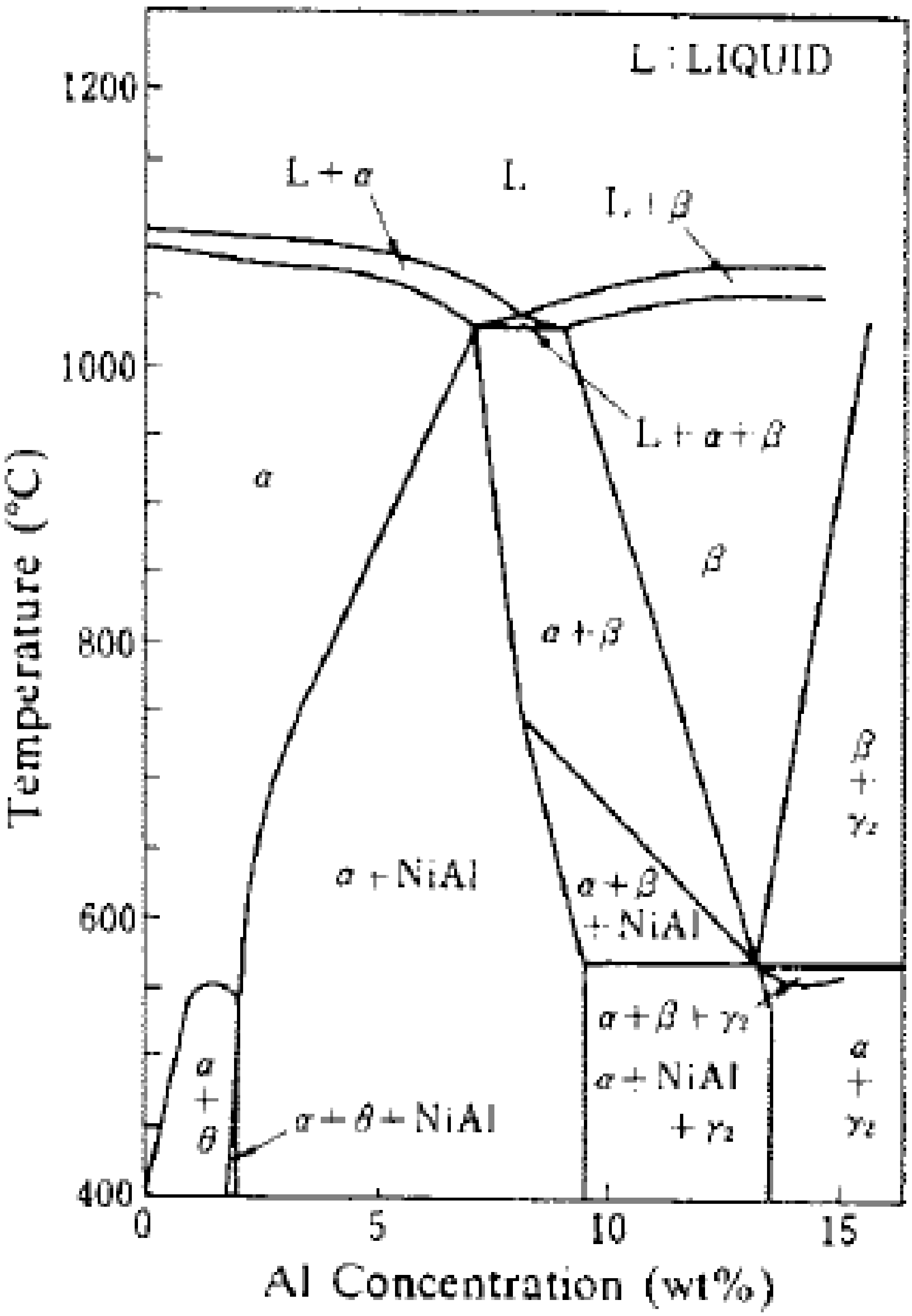

Figure 2.16. a ternary shape memory alloy of Cu-Al-Ni, the vertical cross-section of 3mass% of Ni and phase diagram of alloy [40].

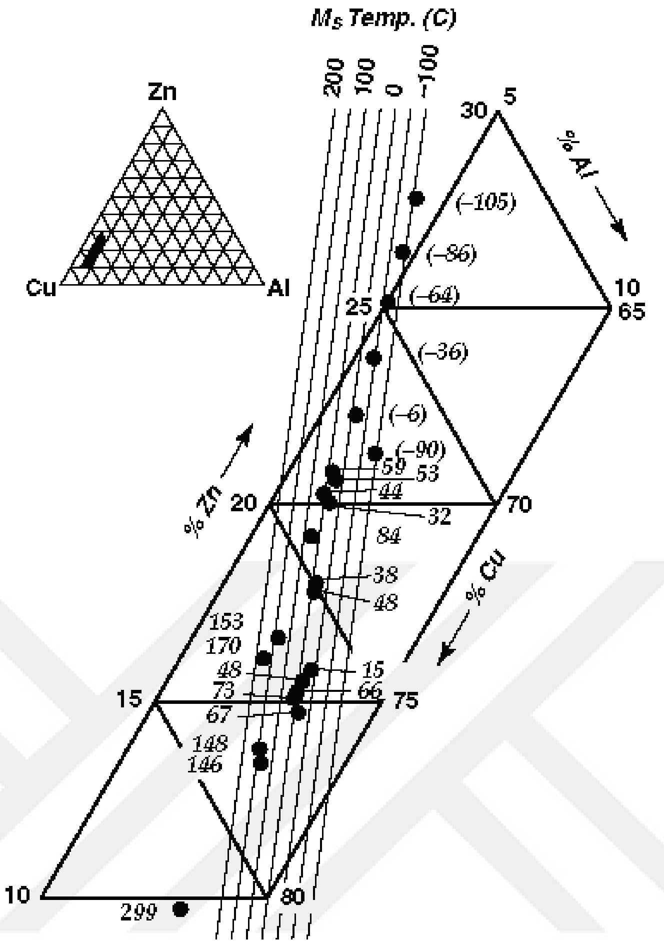

Figure 2.17. The martensite start temperature as a function of composition for Cu-Zn-Al ternary alloys [41].

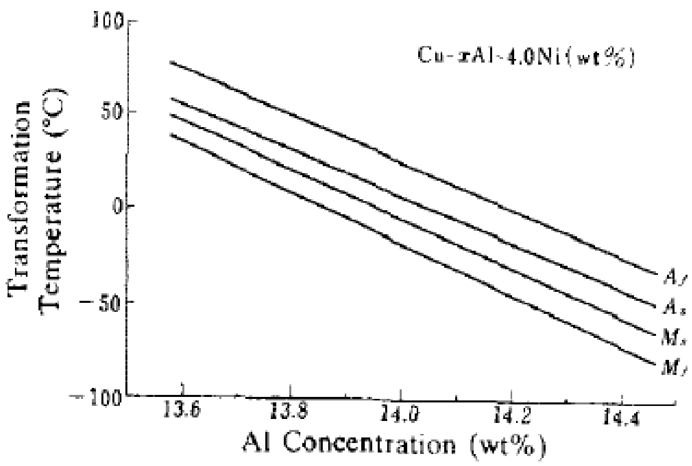

Figure 2.18 In ternary Cu-Al-Ni shape memory alloy, the relation between Al content and transformation temperature [42].

controlling transformation temperature is the composition of the alloy. Also, there are some other factors that significantly affected the transformation temperature like grain size, heat treatment, the number of transformation cycle and quenching rate.

2.7. CuAlNi shape memory alloy

Copper-Aluminum-Nickel is a ternary shape memory alloys materials that most distinguish use from the class of copper-based alloys because this alloy has good thermal stability, high transformation temperature, good thermal and electrical conductivity, and great recoverable strain [43]. This alloy now used in the application of load endure high temperature because of this alloy only one of shape memory alloy of copper-based materials that available at this time. Although Cu-Al-Ni alloy displays little strain recovery percentage [44] and so crisp in the polycrystalline state. Normally the ratio of nickel in this system alloys about 4 wt.% and by adding a nickel to copper aluminum alloy increasing the transformation of the system and reducing the crisp of the system and vice versa.

Copper-Aluminum-Nickel with compare to Copper-Zinc-Aluminum zinc is lesser prone to being aging but copper-aluminum-nickel restricted formability because of their crispness. Some elements of alloying and the way of processing have an effect on the properties of engineering and shape memory on Cu-Al-Ni alloy. Elements like vanadium, Zirconium, Boron and Titanium with microalloying is a technique of powder metallurgy and speed solidification process that doing for improving mechanical properties and ductility of Copper-Aluminum-Nickel polycrystalline alloy [45]. The influence of different alloying materials on mechanical properties and microstructure on this alloy was reviewed by Saud et al [46]. Also, some other people worked about the influence of adding Zirconium and Titanium on these alloys like Brown and Sure [47], Wayman and Lee [48], and Sugimoto et al [47]. The concentrate of Wayman and Lee is about the influence of zirconium and titanium on martensite temperature start on Cu-Al-Ni after added to the alloy, Brown and Sure and Sugimoto et al work display limited develop of grain and grain refinement what happens on these after adding titanium and zirconium.

The influence of adding boron and manganese on stress concentrations comfort at grain boundaries and grain refinement was reported by Wayman and Lee. Also in some studies showed that by addition of Beryllium [49] to the alloy increasing in recoverable strain and fatigue life, and by adding Boron [50] to the alloy increasing ductility of the alloy. Another effect that noted on the properties of shape memory and engineering is processing routes. By melting spinning produced nanostructured Copper-Aluminum-Nickel that display structure stability and good shape memory properties attributed to spacious dislocation densities, which provide many heterogeneous sites of nucleation for formation martensite [51]. The stripes of copper-aluminum-nickel shape memory alloy prepared by warm densification rolling that subjected to the experience of heat treatment negligible growth of the grain and enhanced mechanical properties attributed to the impact of pinning of Nano-sized aluminum oxide separate on grain boundaries [52]. Considerably enhanced on shape memory strain, ductility and great superelastic also reported by Chen et al [53]. In copper-aluminum-nickel shape memory alloys that were usually crisp when liquid phase wire forming technique in the process of production was employed.

3. MATERIALS AND EXPERIMENTAL PROCEDURE

3.1. Materials

In this thesis, $Cu_{79}Al_{12}Ni_{4}Nb_{5}$ (% in wt.) quaternary shape memory was used. This alloy was produced by using high pure of copper (Cu), aluminum (Al), nickel (Ni), niobium (Nb) elements. The powders of these alloys were mixed and then pelletized. The pelletized powder was melted by using arc melter furnace under vacuum. The melting procedure was made several times to ensure the homogeneity of CuAlNiNb alloy.

Figure 3.1. Furnace for aging alloys (PROTHERM).

3.2. Annealing Process

The aim of this thesis to applied annealing on to CuAlNiNb alloys for different hours at 800 ^{o}C temperature (Figure 3.1). Alloys pieces were prepared by using a cutting machine and these pieces were divided into six groups to apply annealing procedure. Table 3.1. gives these six groups and summarizes applying procedure, including the temperature of aging, time of aging, and quenching medium.

Table 3.1. The summary of the applied procedure on CuAlNiNb shape memory alloy.

Alloys' code	Temperature (K)	Time (hours)	Quenching procedure
As cast	----	----	-----
1hr	1073	1	Ice brined
2hr	1073	2	Ice brined
3hr	1073	3	Ice brined
6hr	1073	6	Ice brined
12hr	1073	12	Ice brined
24hr	1073	24	Ice brined

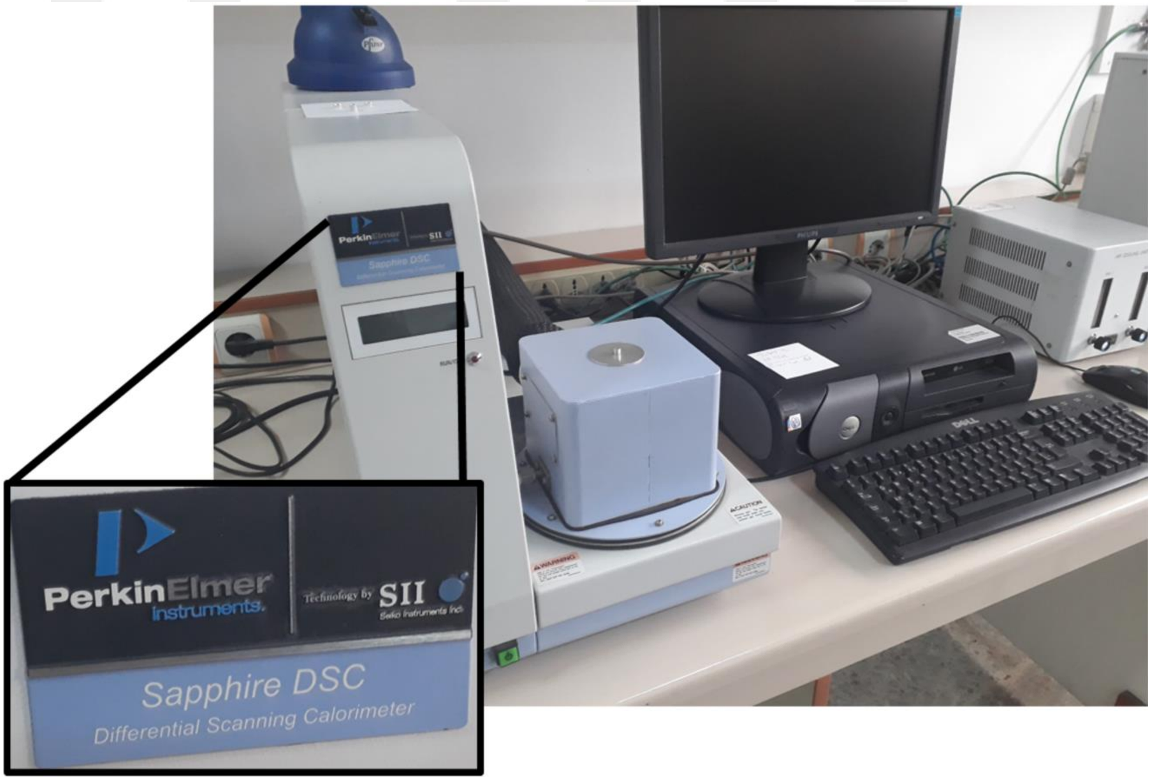

Figure 3.2. Differential Scanning Calorimetry (Perkin Elmer Sapphire).

3.3. Characterization Processes

3.3.1. Transformation Temperature and Thermodynamics Parameters Analysis

Perkin Elmer Sapphire (Figure 3.2) Differential Scanning Calorimetry (DSC) was used to determine martensite and austenite transformation temperature and enthalpy-entropy change of annealed CuAlNiNb shape memory alloy. DSC measurements were made at the heating/cooling rate of 10 ^{o}C/min. in a pure nitrogen atmosphere.

3.3.2. Crystal Structure Analysis

The crystal structure of as-cast and annealed CuAlNiNb shape memory alloys were determined by using Rigaku X-ray Diffractometer (Figure 3.3). The x-ray measurements were made at room temperature by scanning rate of 6 ^{o}/min.

Figure 3.3. X-Ray Diffraction device (RIGAKU D / MAX-B GEIGERFLEX).

3.3.3. Microstructure Analysis

The one-piece of all CuAlNiNb quaternary alloys (as cast and annealed) was molded by using polyester resin to polish as easily. The mold alloys polished by using different sizes of polish paper and silk by using diamond cream. After well polishing, the alloys subjected to etching solvent (5g Fe2Cl-H2O/96 ml ethanol/20 ml HCl acid) to determine the microstructure of alloys. Optical microscopy (PRIOR Model -N334 Incident Light Metallurgical Trinocular Microscope, Figure 3.4) were used to investigate microstructures of Etched CuAlNiNb quaternary alloys at room temperature.

Figure 3.4. PRIOR Model -N334 Incident Light Metallurgical Trinocular Microscope.

4. RESULTS AND DISCUSSION

Figure 4.1. shows the map of constituents distribution in the as-casted CuAlNiNb shape memory alloy. The Cu elements distributed uniformly except in some particular locations. It can be seen that Nb formed star-like shape and some irregular forms that are exactly occupy Cu-free locations, i.e. Cu had not dissolved in Nb phases. While aluminum (Al) are exist with Nb phase. Additionally, nickel (Ni) distributed uniformly in both matrix (Cu) and second phase (Nb-rich phase).

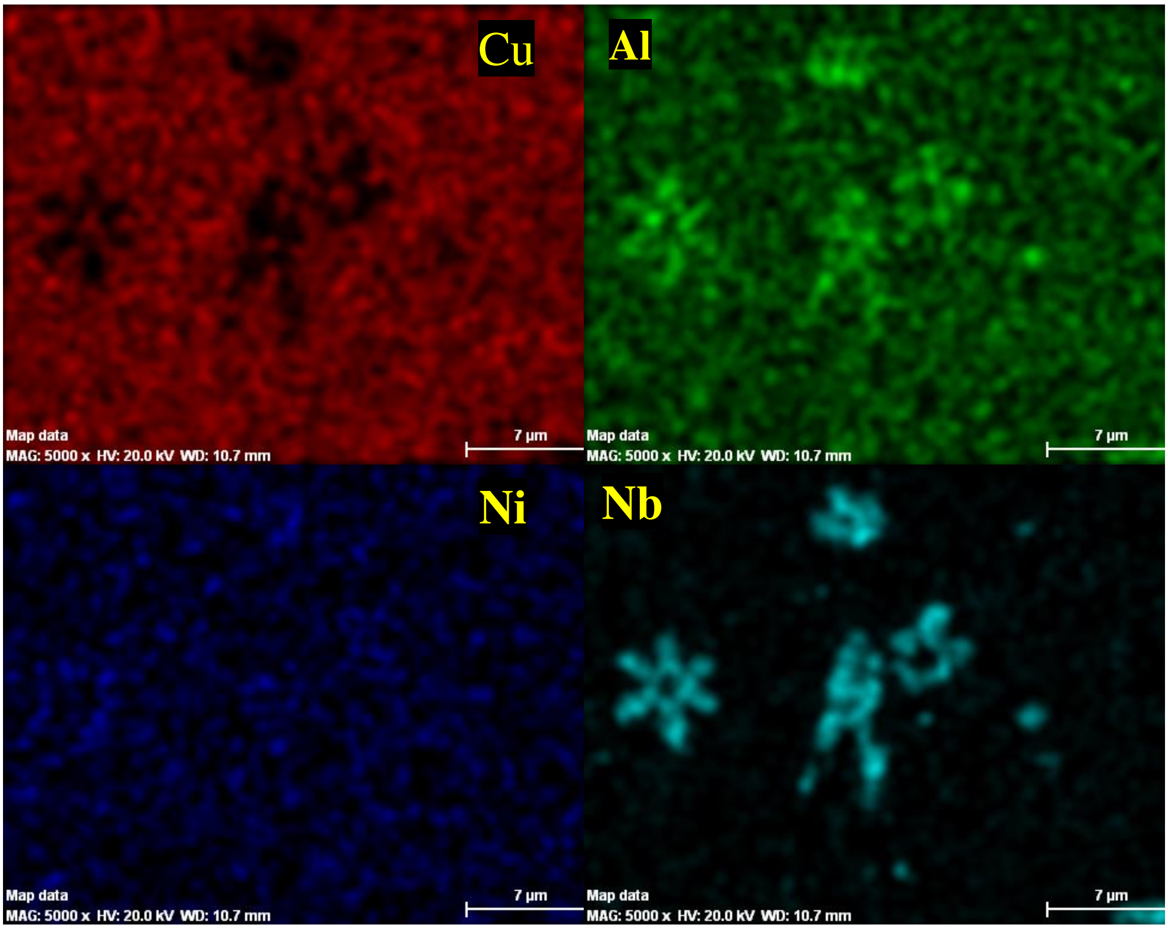

Figure 4.1. Map of compositional distributions of the as-casted Cu-Al-Ni-Nb alloy.

The characteristics of the alloy have classified into the thermal analysis, microstructure, and crystal structural analysis. The effect of thermal treatment for different time aging has been demonstrated in term of graphs and tables, besides some related calculations has been done. In addition, the results have compared with the related literature to support the outcomes of this study.

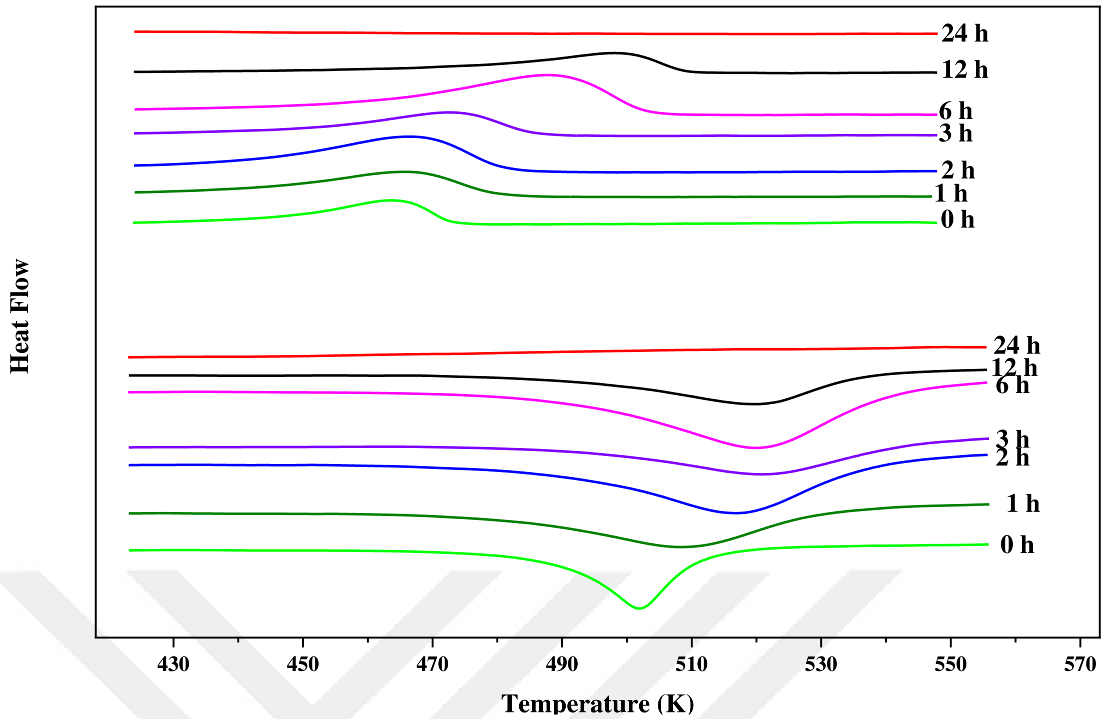

Figure 4.2. The DSC results.

4.1. Thermal Analysis Results

One of the important parts of this study is the phase transformation analysis, which has been investigated using Differential Scanning Calorimetry (DSC). Figure 4.2 shows the DSC results of quaternary CuAlNiNb shape memory alloy. The as-casted alloy shows phase transformation 400K, which can be classified as high-temperature shape memory alloys [18, 54]. It can be seen that the phase transformation, in either austenite transformation (endothermic or heating process) or martensite phase transformation (exothermic or cooling process), has shifted to the higher temperature by keeping the alloy for more hours in the furnace. Since the entire alloys were quenched in the same liquid (in 273.15 K) and all of them were kept at 1073K, then the only reason behind this shift can be described through the microstructural point of view. Also, the phase transformation is a single step transformation, i.e., there is no additional peak, but the austenite and martensite peaks.

In addition, it is found that the alloy has lost its shape memory characteristic when it was kept for 24 h in 1073K. Figure 4.3 illustrates a complete cycle of DSC result for Cu-Al-Ni-Nb shape memory alloy. Since there is not indictable trough or peak in the heating and cooling process for the determined temperature, then it can be concluded that the alloy has completely lost its functionality. Mazzer et al. [55] time of aging straightly effect on the Cu-Al-Ni-Mn shape memory alloy. They examined their sample for 15, 30 and 60 min, where the martensitic phase transformation shifted to the higher temperature. Furthermore, they found that the phase transformation temperatures moved to a higher temperature by increasing the aging temperature.

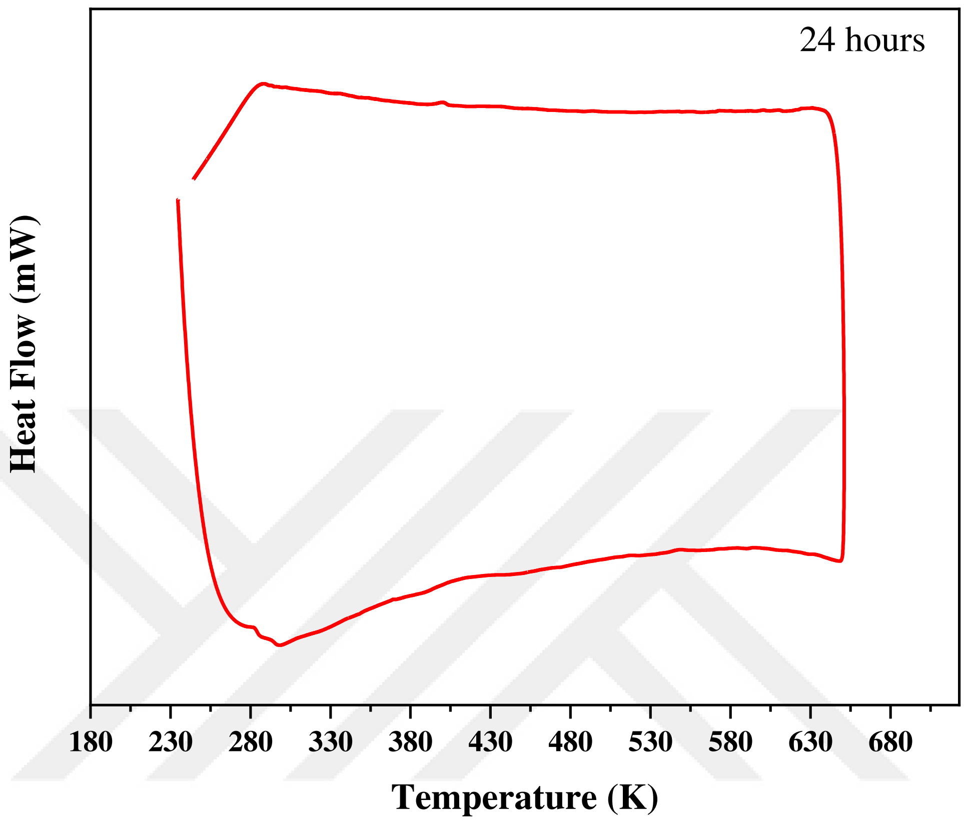

Figure 4.3. The DSC result of the alloy aged for 24 h.

Table 4.1. Phase transformation temperatures in all cases.

Name	A_s (K)	A_p (K)	A_f (K)	M_s (K)	M_p (K)	M_f *(K)*
0h	481.2	501.8	512.4	473.2	464.4	436.5
1h	469.1	508.6	541.2	480.7	465.4	427.9
2h	477.3	517.3	546.9	481.2	466.8	435.6
3h	479.7	521.4	549.5	485.9	472.8	437
6h	479.4	520.3	556	503.6	489	456.1
12h	478.5	520.3	545.2	509.3	498.4	473.8
24h	----	------	------	-------	-----	-----

Table 4.1 represents the phase transformation obtained from the DSC results. When the SMA heated, in some particular temperature it began to transform from martensite (M) to austenite, which is known as austenite start (A_s). Then the transformation reached the maximum

that showed DSC peak and it labeled as austenite peak (A_p). The austenite transformation process finished in another temperature, which is known as austenite finish temperature (A_f). Likewise, for the heating process the alloy transformed from austenite to martensite that gave three transformation temperatures, including martensite start (M_s), martensite peak (M_p), and martensite finish (M_f) temperatures [56, 57].

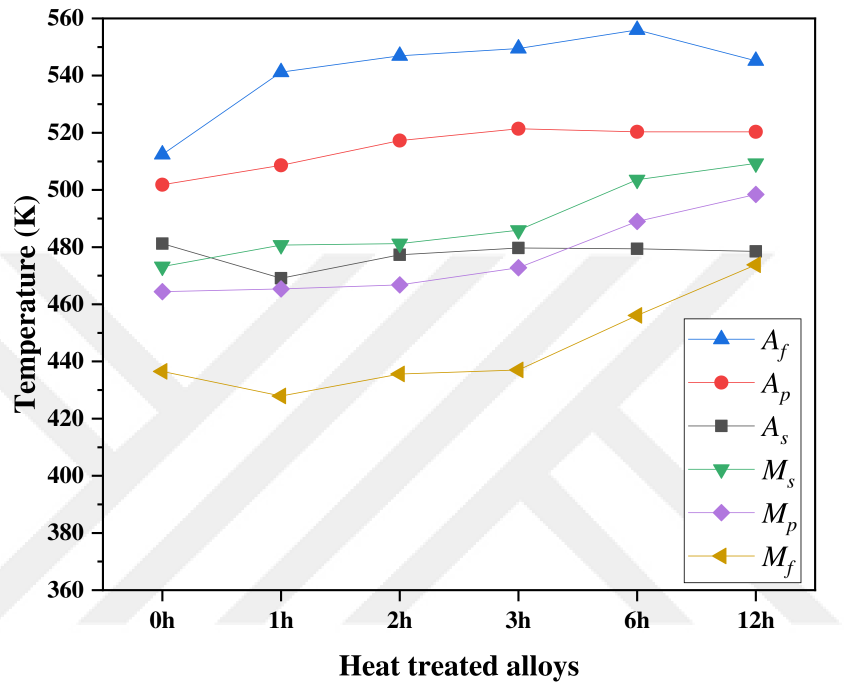

Figure 4.4. Phase transformation temperatures for all cases.

Table 4.2. Enthalpy and entropy change obtained for all heat-treated samples.

Name	$\Delta H_{M\rightarrow A}$ (J/g)	$\Delta H_{A\rightarrow M}$ (J/g)	$\Delta S^{M\rightarrow A}$ (J/kg K)	$\Delta S^{A\rightarrow M}$ (J/kg K)
0h	10.7	9.49	21.71266	19.25731
1h	10.2	9.36	19.96281	18.31882
2h	10	8.72	19.45336	16.96333
3h	10.4	8.47	20.08885	16.36083
6h	6.79	8.83	12.81616	16.66667
12h	7.26	10	13.76956	18.96633
24h	----	---	------	-------

It can be obviously seen that all phase transformation temperatures increased by increasing the time of aging (Figure 4.4). Moreover, since for all aged specimens austenite start value is less than martensite start temperature, then the alloy can be classified as second class (Class II) of shape memory alloys [58-60].

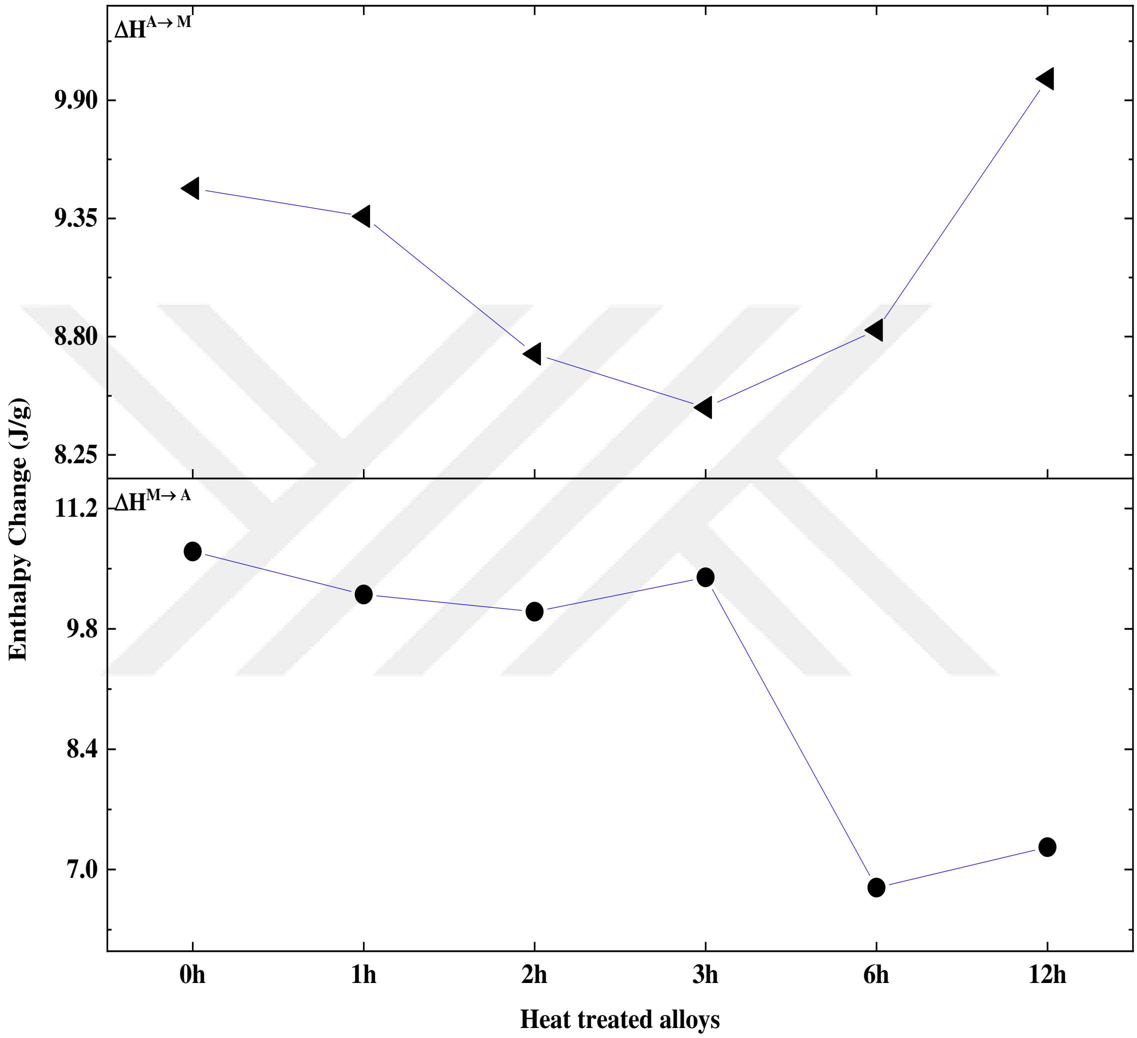

Figure 4.5. The enthalpy change for all various aging samples

The peak obtained in heat flow vs. temperature graph can be handled for calculating heat capacity or latent heat of phase transformation, known as enthalpy change (ΔH). These values (for the endothermic and exothermic process) mathematically represented by integrating the area under the martensitic process. However, the values were found by the corresponding DSC software. Figure 4.5 shows that enthalpy change decreased by increasing time of aging. The value of enthalpy for martensite phase transformation increased for aging more than 3 hours.

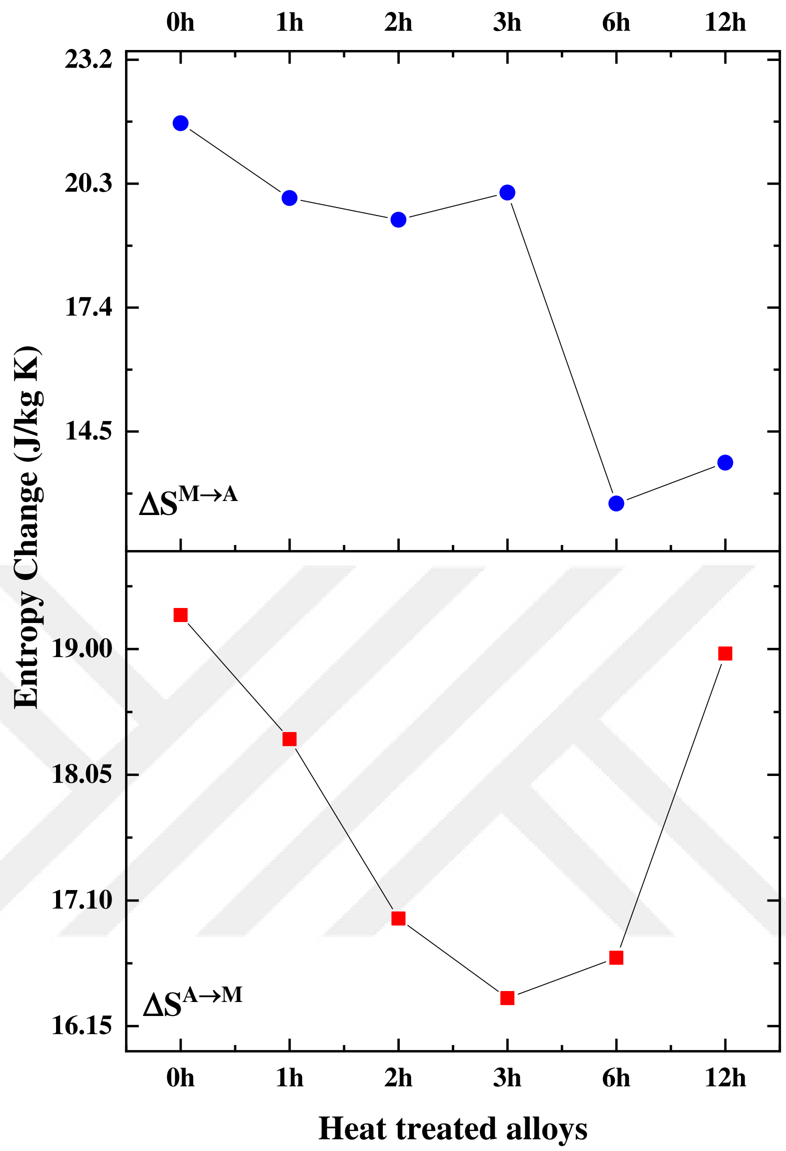

Figure 4.6. Entropy change of all investigated specimens.

The enthalpy change value can help to calculate entropy change of the phase transformation using the following equation [54, 61, 62]:

$$\Delta S^{M\rightarrow A} = \int_{A_s}^{A_f} \frac{dq}{dT}\left(\frac{dT}{dt}\right)^{-1} dT$$

or

$$\Delta S^{M\rightarrow A} = \int_{A_s}^{A_f} \frac{dQ^{M\rightarrow A}}{T_o} = \frac{\Delta H^{M\rightarrow A}}{T_o} \tag{4.1}$$

The Eq. (4.1) gives can be rearranged such that [63]:

$$\Delta S^{A(M)\to M(A)} = T_o \Delta H^{A(M)\to M(A)} \tag{4.2}$$

The Eq. (4.2) gives the entropy change for the heating process, where the martensite phase transforms to the austenite phase. The same calculation can be accomplished for the reverse transformation process such that the enthalpy change for austenite phase transformation ($\Delta H^{M\to A}$) substituted by enthalpy change for martensite phase transformation ($\Delta H^{A\to M}$). Figure 4.6 presents the entropy changes obtained by Eq. (4.2). Generally, the aging time decreased the entropy for both forward and reverse phase transformation process. For martensite phase transformation, the sample with 3 hours of aging shows the minimum entropy change.

It should be pointed out that according to the second law of thermodynamics, the entropy change of a process must always be equal or greater than zero ($\Delta S \geq 0$). Therefore, it should be taken into account that all temperature converts to the Kelvin scale (K), and the enthalpy change (even for reversible phase transformation) concerned as a positive value.

The other unknown parameter that should be first obtained is the equilibrium temperature (T_o). The mathematical representation for T_o is as follows [64-66]:

$$T_o = \frac{M_s + A_f}{2} \tag{4.3}$$

The calculated equilibrium temperature is illustrated in Figure 4.7, where its value dramatically increased after 1 hour aged at 1073K. Also, for the other specimens the T_o continuously increased up to 6 hours, then it decreased for 12 hours aging. The value T_o can be obtained using the average of martensite start and austenite finish temperature values. However, since there was no phase transformation occurred for 24h aged sample, so there is no equilibrium temperature for this case.

Free enthalpy [67] or Gibbs free energy is the amount of energy that necessary for doing the phase transformation, and it can be calculated for a constant temperature. The following equation gives the value of Gibbs free energy at equilibrium temperature, where both exothermic and endothermic reactions are equal to zero:

$$\begin{aligned}\Delta G^{M\to A}(T_o) &= G^A(T_o) - G^M(T_o) = (H^A - T_o S^A) - (H^M - T_o S^M) \\ &= \Delta H^{M\to A} - (T_o \Delta S^{M\to A}) = 0\end{aligned} \tag{4.4}$$

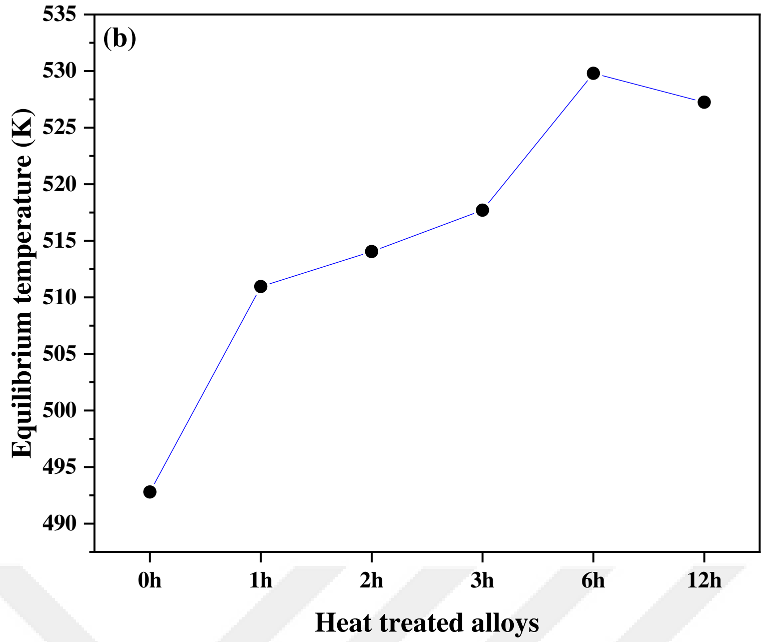

Figure 4.7. Equilibrium temperature for the Cu-Al-Ni-Nb alloy.

Table 4.3. Temperature hysteresis (H_t), equilibrium temperatures (T_o), Gibbs free energy (ΔG) for martensite phase transformation ($\Delta G^{A\to M}$), and elastic energy (G_E) of the alloys.

Name	Temperature Hysteresis (K)	T_o (K)	$\Delta G^{A\to M}$ (J)	G_E (J)
0h	37.4	492.8	425.5682	706.7431
1h	43.2	510.95	603.8751	967.2336
2h	50.5	514.05	639.0429	773.5279
3h	48.6	517.7	638.8256	800.0444
6h	31.3	529.8	335.7833	791.6667
12h	21.9	527.25	247.1636	673.3049
24h	-------	------	------	-------

The Eq. (4.4) represents the change of Gibbs free energy, which is the difference between austenite (G^A) and martensite (G^M). Since the Gibbs free energy is energy of non-expanded work, so it equal to ($H^A - T_o S^A$), for austenite, and ($H^M - T_o S^M$), for martensite. For the martensite phase transformation, the Eq. (4.4) can be written as:

$$\Delta G^{A\to M}(M_s) = \Delta G^{M\to A}(T_o) - \Delta G^{M\to A}(M_s) \quad (4.5)$$

or

$$\Delta G^{A\to M}(M_s) = -(T_o - M_s)\Delta S^{M\to A} \quad (4.6)$$

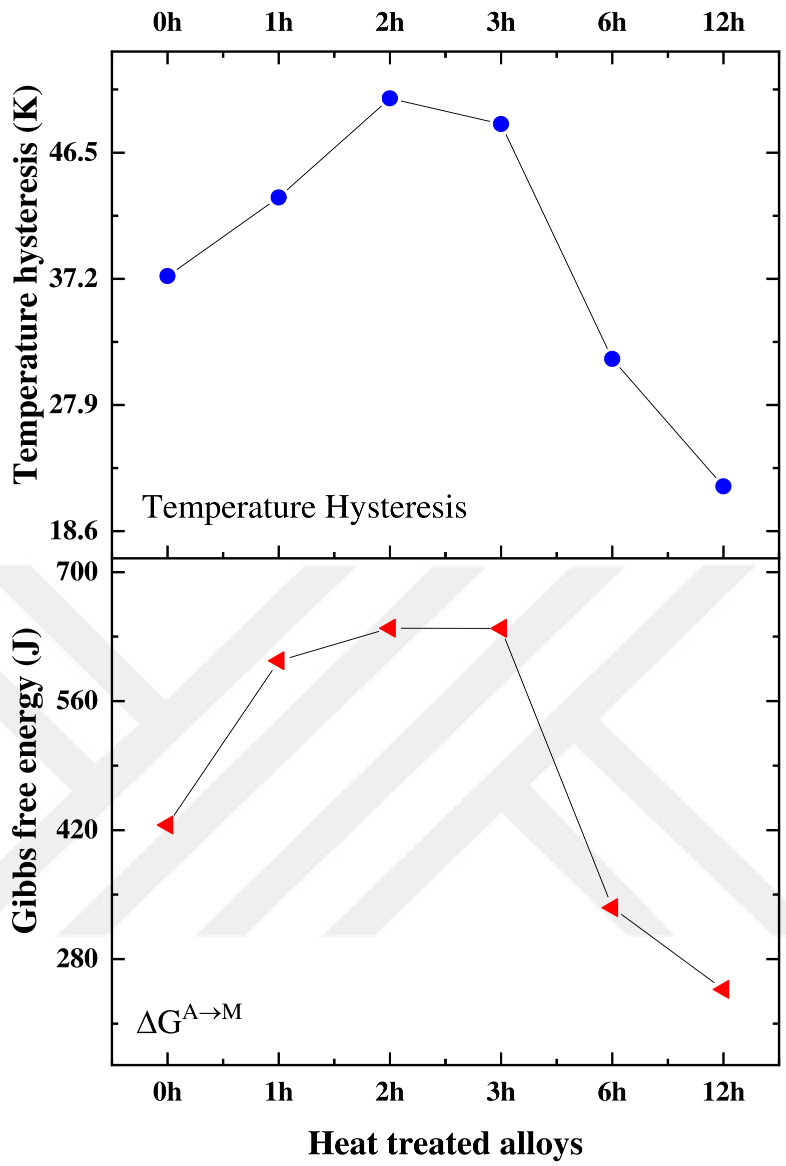

Figure 4.8. Gibbs free energy and temperature hysteresis for all cases.

The calculated value of Gibbs free energy is listed in Table 4.3. In Figure 4.8, it can be seen that temperature hysteresis (H_t=A_f - M_s) and Gibbs free energy for martensite phase transformation have the same pattern., Firstly, these physical parameters have increased for the two hours aging and then dramatically decreased with increasing aging time. On the other hand, since there was no data for the 24h aged sample, H_t it has not taken into account.

The subtraction between Gibbs free energy of martensite phase transformation and austenite phase transformation can give elastic energy that can be expressed as the following mathematical formula [54]:

$$G_e = \Delta G^{A\to M}(M_s) - \Delta G^{A\to M}(M_f) = (M_s - M_f)\Delta S^{M\to A} \tag{4.7}$$

Figure 4.9 showed the calculated elastic energy values as a function of aging time of the Cu-Al-Ni-Nb SMA. The alloy showed maximum elastic energy for one hour aging at 1073K. However, it decreased again and almost stayed constant for 2h, 3h, and 6h. The G_e decreased again for 12h and for the last specimens (24h) no result has been achieved.

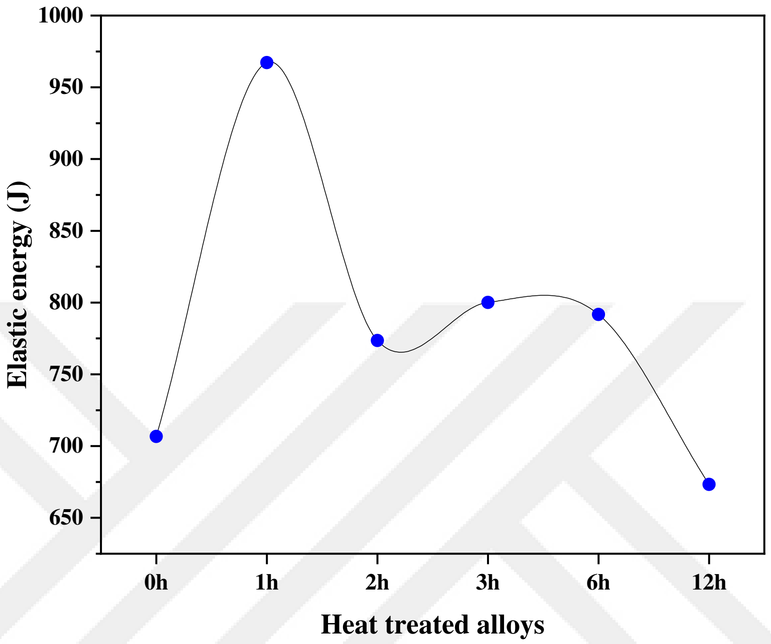

Figure 4.9. Elastic energy of the Cu-Al-Ni-Nb SMA in different aging time.

Figure 4.10 illustrats the XRD results of the as-casted and heat treatment as a function of time. The XRD patterns was affected by the duration of aging. In the as-casted alloy there is a single peak, which belongs to martensite (β_1') phase and the heat treatment created multi phases in the alloy. Generally, the matrix was found to be martensite (β_1') with some other precipitated phase, including γ', α, and β_1, where α, and β_1 are metastable austenite phases and γ' is another martensite phase with different crystal structure.

The peak intensities increased by increasing the time of aging. After three hours of aging the intensities of the peaks decreased againg. Additionally, no γ'phase can not be found in the 24h sample.

The nanocrystallin of the alloys can be found using Schrerre equations and the x-ray differaction patterns. The Schrerer equation is as follows [57, 68]:

$$D = \frac{0.9\,\lambda}{B\cos\theta} \qquad (4.8)$$

where λ is the x-ray wavelength, which is equal to 1.5406 Å, B is the full width at half maximum (FWHM) for the XRD peaks, and θ is the Braggs angle.

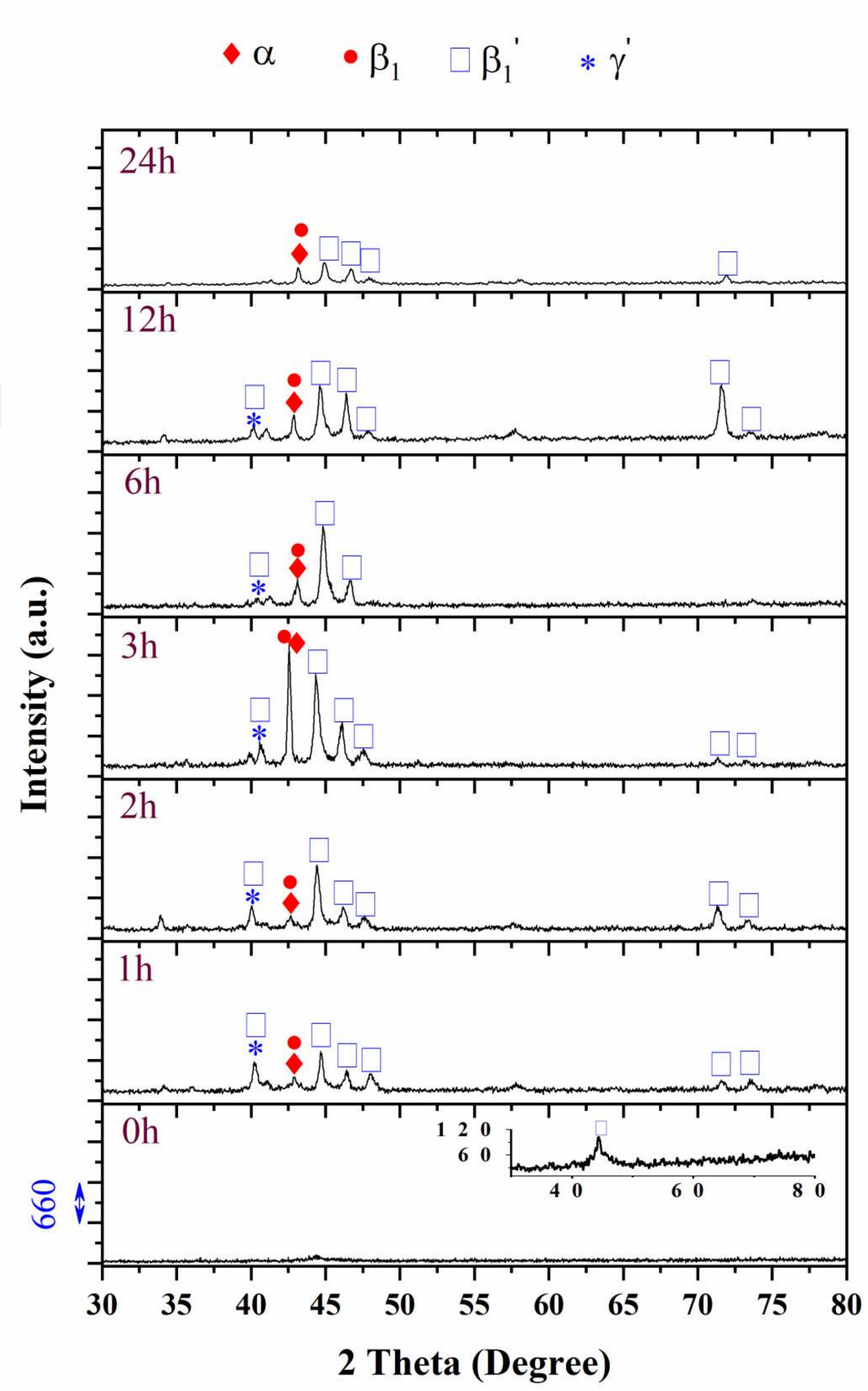

Figure 4.10. The XRD results of the as-casted and all heat treated alloys.

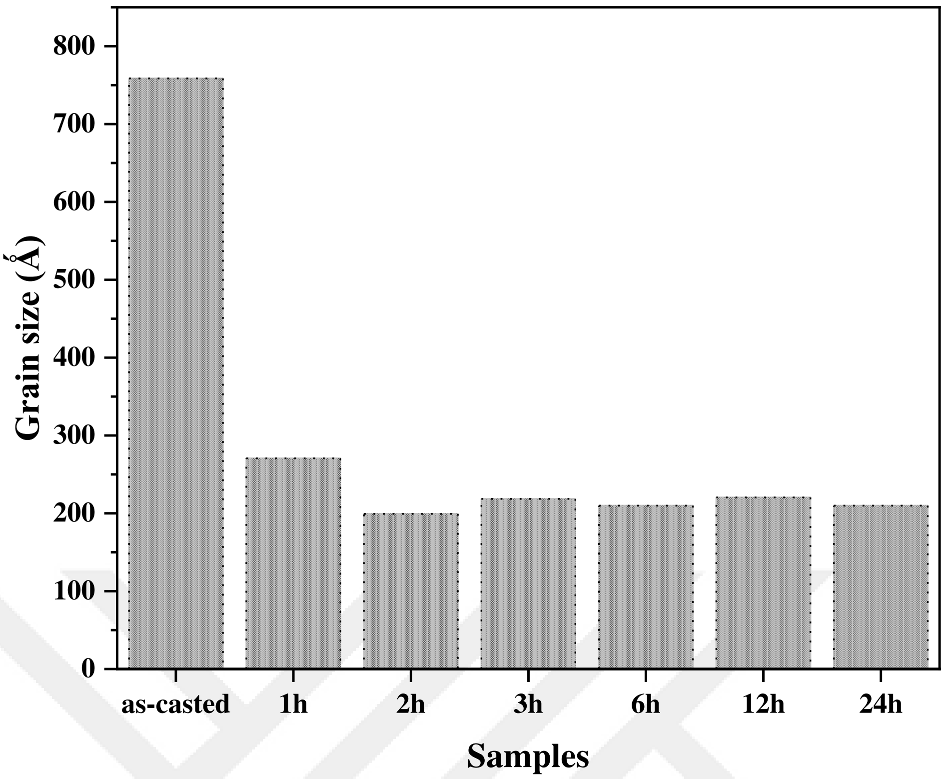

Figure 4.11. The nano grain size of all specimens.

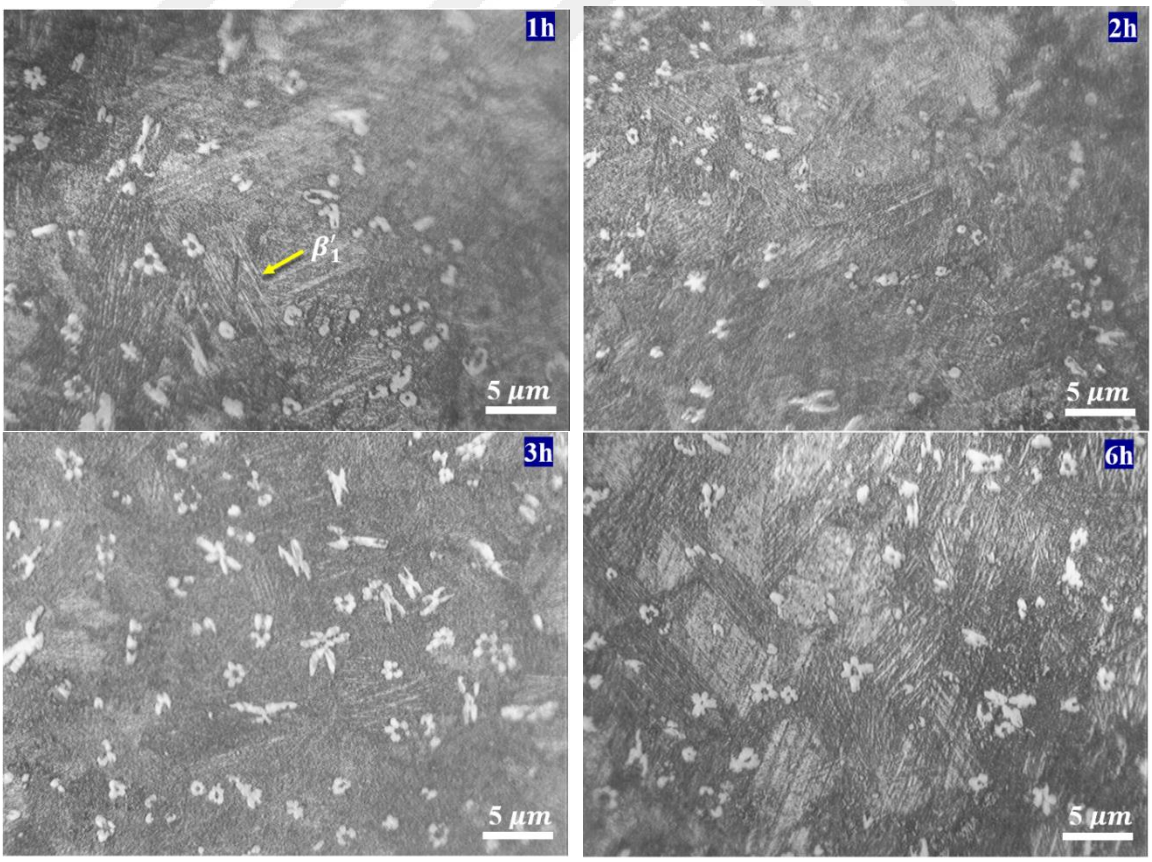

Figure 4.12. The optical microscope images of as caseted and aged alloys.

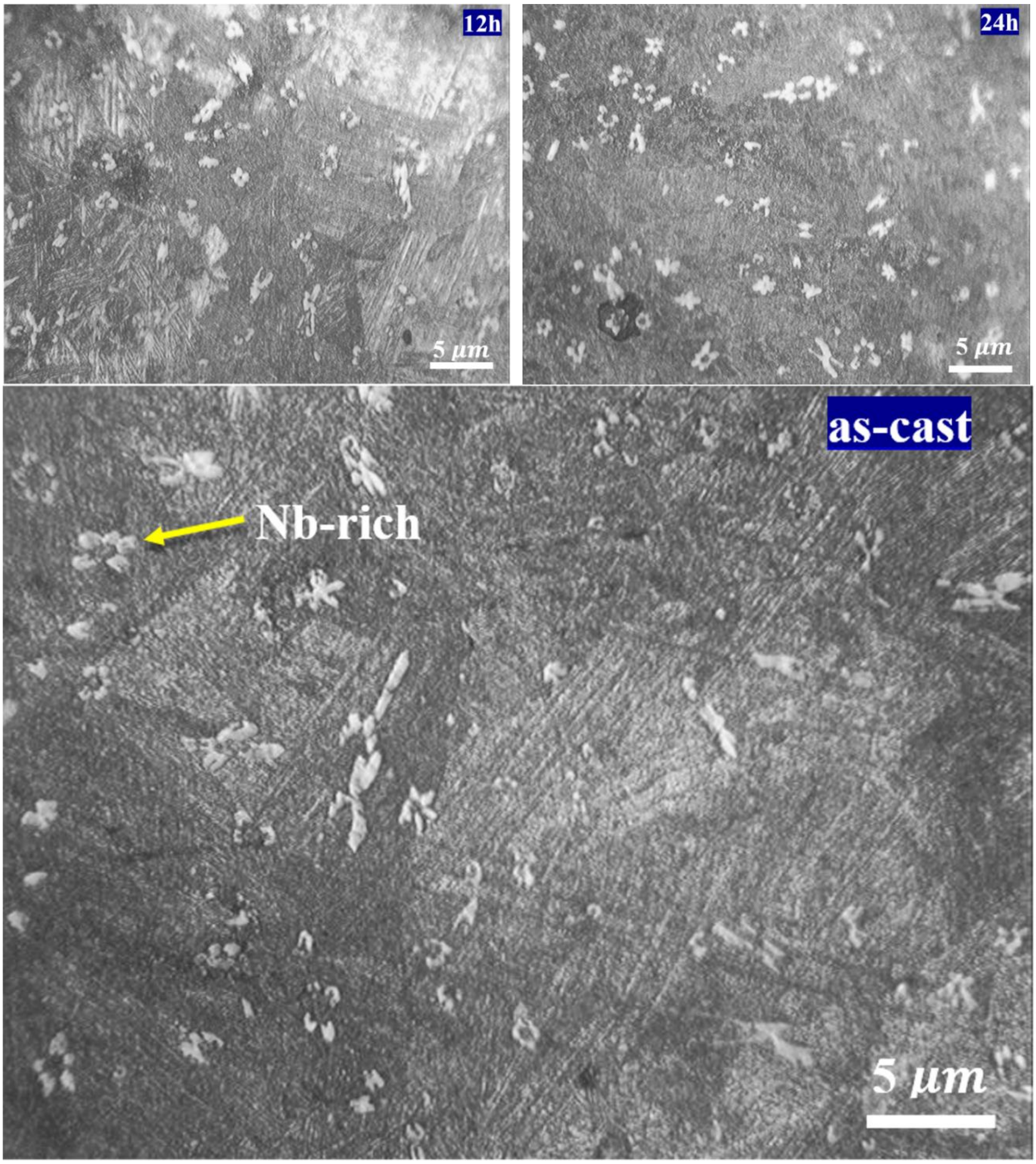

Figure 4.12. The optical microscope images of as caseted and aged alloys (continoue)

Figure 4.11 illustrates the calculated nano crystallites of the as-casted and aged specimens. It is obviously can be seen that the crystallite sizes were affected by the aging process. However, Shakir et al. [69] showed that the grain sizes of CuAlNi-Mn SMA aged for 1, 2, 3, 4, and 5 hours increased with increasing time of aging and the temperature of aging.

Figure 4.12 showed optical microscopt images. In both as-casted and aged alloys there are many flower-like precipitated phases that found to be Nb-rich phases. Also, there is nidle shaped martensite β_1' phases that is the matrix phases of the alloys.

5. CONCLUSION

In this study, a single homogenous shape memory alloy was produced by arc melting in an argon atmosphere. The quaternary alloy consisted of (79.0 wt. %) copper-(13.0 wt. %) aluminum-(3.0 wt. %) nickel-(5.0 wt. %) niobium prepared from high pure powder metallic elements. Seven small pieces were cut from the as-casted ingot for applying heat treatment. The aging process was performed for 0, 1, 2, 3, 6, 12, and 24 hours in 1073K. Some thermal, microstructural, and other physical parameters were examined using differential scanning calorimetry, metallurgical Microscope, and x-ray diffraction equipment. The important outcomes of this investigation are as follows:

- The map of compositional elements showed that neither copper nor niobium did not dissolved to each other. Nickel is distributed uniformly all over the sample, while aluminum contributed in the Nb-riched phase less than the matrix phase.
- All testes samples were showed high temperature shape memory alloy characteristics.
- The martensite and austenite phase transformation temperatures were shifted to a high temperature by increasing the time of aging.
- The alloy was lost its shape memory properties when they kept in the furnace for 24 hours.
- The enthalpy and entropy changes of martensite phase transformation were decreased by increasing the aging temperature, but for the alloys that were kept for more than 3h at 1073K, both ΔH and ΔS again started to increase. It is also, noticed that since the sample with 24 h aging did not show transformation temperatures, then it has not enthalpy and hence its entropy change value was not obtained.
- The value of equilibrium temperature was increased by aging time.
- In opposite to enthalpy and entropy changes, the Gibbs free energy and elastic energy of the alloy were increased up to 3h aging time, however, after that time it started to diminish.
- The XRD patterns were affected by applying heat treatment on the alloys.

REFERENCES

[1] Sater, J.M. *Smart Structures and Materials 1997: Industrial and Commercial Applications of Smart Structures Technologies*. in *Smart Structures and Materials 1997: Industrial and Commercial Applications of Smart Structures Technologies*. 1997.

[2] Otsuka, K. and Wayman, C. (1998). Mechanism of shape memory effect and superelasticity, *Shape memory materials*, C, 27-48.

[3] Huang, W. (2002). On the selection of shape memory alloys for actuators, *Materials & design*, C 23, 11-19.

[4] Jani, J.M., Leary, M., Subic, A., and Gibson, M.A. (2014). A review of shape memory alloy research, applications and opportunities, *Materials & Design (1980-2015)*, C 56, 1078-1113.

[5] Wu, M.H. and Schetky, L. *Industrial applications for shape memory alloys*. in *Proceedings of the international conference on shape memory and superelastic technologies*. 2000.

[6] Hautcoeur, A. and Eberhardt, A., *Eyeglass frame with very high recoverable deformability*, 1997, Google Patents.

[7] Jani, J.M., Leary, M., and Subic, A. (2014). Shape Memory Alloys in Automotive Applications, *Applied Mechanics & Materials*, C.

[8] Stoeckel, D. (1990). Shape memory actuators for automotive applications, *Materials & design*, C 11, 302-307.

[9] Van Humbeeck, J. (1999). Non-medical applications of shape memory alloys, *Materials Science and Engineering: A*, C 273, 134-148.

[10] Bil, C., Massey, K., and Abdullah, E.J. (2013). Wing morphing control with shape memory alloy actuators, *Journal of Intelligent Material Systems and Structures*, C 24, 879-898.

[11] Schetky, L.M. (1991). Shape memory alloy applications in space systems, *Materials & design*, C 12, 29-32.

[12] Petrini, L. and Migliavacca, F. (2011). Biomedical applications of shape memory alloys, *Journal of Metallurgy*, C 2011.

[13] Morgan, N. (2004). Medical shape memory alloy applications—the market and its products, *Materials Science and Engineering: A*, C 378, 16-23.

[14] Mantovani, D. (2000). Shape memory alloys: Properties and biomedical applications, *Jom*, C 52, 36-44.

[15] Sun, L. and Huang, W. (2009). Nature of the multistage transformation in shape memory alloys upon heating, *Metal Science and Heat Treatment*, C 51, 573-578.

[16] Es-Souni, M., Es-Souni, M., and Fischer-Brandies, H. (2005). Assessing the biocompatibility of NiTi shape memory alloys used for medical applications, *Analytical and bioanalytical chemistry*, C 381, 557-567.

[17] Wayman, C. (1980). Some applications of shape-memory alloys, *Jom*, C 32, 129-137.

[18] Qader, I.N., Kök, M., and Dağdelen, F. (2019). Effect of heat treatment on thermodynamics parameters, crystal and microstructure of (Cu-Al-Ni-Hf) shape memory alloy, *Physica B: Condensed Matter*, C 553, 1-5.

[19] Dagdelen, F., Aldalawi, M., Kok, M., and Qader, I. (2019). Influence of Ni addition and heat treatment on phase transformation temperatures and microstructures of a ternary CuAlCr alloy, *The European Physical Journal Plus*, C 134, 66.

[20] Yoshizawa, Y.a., Oguma, S., and Yamauchi, K. (1988). New Fe-based soft magnetic alloys composed of ultrafine grain structure, *Journal of applied Physics*, C 64, 6044-6046.

[21] Amini, R., Mousavizad, S., Abdollahpour, H., Ghaffari, M., Alizadeh, M., and Okyay, A.K. (2013). Structural and microstructural phase evolution during mechano-synthesis of

nanocrystalline/amorphous CuAlMn alloy powders, *Advanced Powder Technology*, C 24, 1048-1053.

[22] Sarı, U. and Kırındı, T. (2008). Effects of deformation on microstructure and mechanical properties of a Cu–Al–Ni shape memory alloy, *Materials characterization*, C 59, 920-929.

[23] Otsuka, K. and Wayman, C.M., (1999). *Shape memory materials*, Cambridge university press,

[24] Duerig, T.W., Melton, K., and Stöckel, D., (2013). *Engineering aspects of shape memory alloys*, Butterworth-Heinemann,

[25] Kurdjumov, G. and Khandros, L. (1949). First reports of the thermoelastic behaviour of the martensitic phase of Au-Cd alloys, *Doklady Akademii Nauk SSSR*, C 66, 211-213.

[26] Buehler, W.J., Gilfrich, J., and Wiley, R. (1963). Effect of low-temperature phase changes on the mechanical properties of alloys near composition TiNi, *Journal of Applied Physics*, C 34, 1475-1477.

[27] Wang, F.E., Buehler, W.J., and Pickart, S.J. (1965). Crystal Structure and a Unique``Martensitic''Transition of TiNi, *Journal of applied Physics*, C 36, 3232-3239.

[28] Schetky, L.M. (1982). Shape-memory alloys, *Kirk-Othmer Encyclopedia of Chemical Technology*, C.

[29] Wu, M.H. and Schetky, L.M. (2000). INDUSTRIAL APPLICATIONS FOR SHAPE MEMORY ALLOYS, *Proceedings of the International Conference on Shape Memory and Superelastic Technologies, Pacific Grove, California*, C, P.171-182.

[30] H.C.Donkersloot and Vucht, J.H.N.V. (1970). Martensitic transformations in gold-titanium, palladium-titanium and platinum-titanium alloys near the equiatomic composition, *Journal of the Less Common Metals*, C 20, 83-91.

[31] Melton, K. and Mercier, O. (1978). Deformation behavior of NiTi-based alloys, *Metallurgical Transactions A*, C 9, 1487-1488.

[32] Miyazaki, S., Mizukoshi, K., Ueki, T., and T. Sakuma, Y.L. (1999). Fatigue life of Ti–50 at.% Ni and Ti–40Ni–10Cu (at.%) shape memory alloy wires, *Materials Science and Engineering: A*, C 273-275, 658–663.

[33] Ullakko, K., Huang, J.K., Kantner, C., O'Handley, R.C., and Kokorin, V.V. (1996)). Large magnetic-field-induced strains in Ni2MnGa single crystals, *Applied Physics Letters*, C 69, 1966–1968.

[34] Karaca, H.E., Karaman, I., Basaran, B., Chumlyakov, Y.I., and Maier, H.J. (2006). Magnetic field and stress induced martensite reorientation in NiMnGa ferromagnetic shape memory alloy single crystals, *Acta Materialia*, C 54, 233-245.

[35] Lagoudas, D.C., (2008). *Shape memory alloys: modeling and engineering applications.*, Springer Science & Business Media,

[36] Otsuka, K. and M.Wayman, C., (1999). *Shape Memory Materials*, Cambridge,, Cambridge University Press

[37] Shuyong, J. and Yanqiu, Z. (2012). Microstructure evolution and deformation behavior of as-cast NiTi shape memory alloy under compression, *Transactions of Nonferrous Metals Society of China*, C 22, 90-96.

[38] Naresh, C., Bose, P.S.C., and Rao, C.S.P. (2016). Shape memory alloys: a state of art review, *Materials Science and Engineering: A*, C 149.

[39] Funakubo, Hiroyasu, and Kennedy, J.B., (1987). *Shape Memory Alloys*, Gordon and Breach Science Publishers,

[40] Dunne, D. and Kennon, N. *AGING OF COPPER-BASED SHAPE MEMORY ALLOYS*. in *Metals Forum*. 1981. PERGAMON-ELSEVIER SCIENCE LTD THE BOULEVARD, LANGFORD LANE, KIDLINGTON ….

[41] Delaey, L., Deruyttere, A., Aernoudt, N., and Roos, J. (1978). Shape Memory Effect, Super-Elasticity and Damping in Cu-Zn-Al Alloys, *Project*, C 238, 68.

[42] Tadaki, T. (1998). Cu-based shape memory alloys, *Shape memory materials*, C, 97-116.

[43] Fugazza, D. (2003). Shape-memory alloy devices for earthquake engineering: Mechanical properties, constitutive modeling and numerical simulations, *Master's Thesis, University of Pavia, Pavia, Italy*, C.

[44] Todorović, A., Rudolf, R., Romčević, N., Đorđević, I., Milošević, N., Trifković, B., Veselinović, V., and Čolić, M. (2014). BIOCOMPATIBILITY EVALUATION OF Cu-Al-Ni SHAPE MEMORY ALLOYS, *CONTEMPORARY MATERIALS*, C 2, 228-238.

[45] Motoyasu, G., Kaneko, M., Soda, H., and McLean, A. (2001). Continuously cast Cu-Al-Ni shape memory wires with a unidirectional morphology, *Metallurgical and Materials Transactions A*, C 32, 585-593.

[46] Saud, S.N., Hamzah, E., and Bakar, T.A.A. (2013). A review on influence of alloying elements on the microstructure and mechanical properties of Cu-Al-Ni shape memory alloys, *Jurnal Teknologi*, C 64.

[47] Sure, G. and Brown, L. (1984). The mechanical properties of grain refined β-cuaini strain-memory alloys, *Metallurgical and Materials Transactions A*, C 15, 1613-1621.

[48] Lee, J. and Wayman, C. (1986). Grain refinement of Cu・ Zn・ Al shape memory alloys, *Metallography*, C 19, 401-419.

[49] Xu, H.P., Song, G.F., and Mao, X.M. *Influence of Be and Ni to Cu-Al Alloy Shape Memory Performance*. in *Advanced Materials Research*. 2011. Trans Tech Publ.

[50] Morris, M. (1991). Influence of boron additions on ductility and microstructure of shape memory Cu・ Al・ Ni alloys, *Scripta metallurgica et materialia*, C 25, 2541-2546.

[51] Izadinia, M. and Dehghani, K. (2011). Structure and properties of nanostructured Cu-13.2 Al-5.1 Ni shape memory alloy produced by melt spinning, *Transactions of Nonferrous Metals Society of China*, C 21, 2037-2043.

[52] Vajpai, S., Dube, R., and Sangal, S. (2011). Microstructure and properties of Cu–Al–Ni shape memory alloy strips prepared via hot densification rolling of argon atomized powder preforms, *Materials Science and Engineering: A*, C 529, 378-387.

[53] Chen, Y., Zhang, X., Dunand, D.C., and Schuh, C.A. (2009). Shape memory and superelasticity in polycrystalline Cu–Al–Ni microwires, *Applied Physics Letters*, C 95, 171906.

[54] Kök, M., Qader, I.N., Mohammed, S.S., ÖNER, E., Dağdelen, F., and Aydogdu, Y. (2020). Thermal Stability and Some Thermodynamics Analysis of Heat Treated Quaternary CuAlNiTa Shape Memory Alloy, *Materials Research Express*, C 7.

[55] Mazzer, E., Gargarella, P., Cava, R., Bolfarini, C., Galano, M., and Kiminami, C. (2017). Effect of dislocations and residual stresses on the martensitic transformation of Cu-Al-Ni-Mn shape memory alloy powders, *Journal of Alloys and Compounds*, C 723, 841-849.

[56] Kok, M., Al-Jaf, A.O.A., Çirak, Z.D., Qader, I.N., and Özen, E. (2019). Effects of heat treatment temperatures on phase transformation, thermodynamical parameters, crystal microstructure, and electrical resistivity of NiTiV shape memory alloy, *Journal of Thermal Analysis and Calorimetry*, C.

[57] Buytoz, S., Dagdelen, F., Qader, I., Kok, M., and Tanyildizi, B. (2019). Microstructure Analysis and Thermal Characteristics of NiTiHf Shape Memory Alloy with Different Composition, *Metals and Materials International*, C, 1-12.

[58] Acar, E., Toker, G.P., Kurkcu, H., and Karaca, H.E. (2019). High temperature shape memory behavior of Ni47. 3Ti29. 7Hf20Pd3 alloys, *Intermetallics*, C 111, 106518.

[59] Dunne, D. and Wayman, C. (1973). The effect of austenite ordering on the martensite transformation in Fe-Pt alloys near the composition Fe 3 Pt: I. Morphology and transformation characteristics, *Metallurgical Transactions*, C 4, 137-145.

[60] Dunne, D. and Wayman, C. (1973). The effect of austenite ordering on the martensite transformation in Fe-Pt alloys near the composition Fe 3 Pt: II. Crystallography and general features, *Metallurgical Transactions*, C 4, 147-152.

[61] Elrasasi, T., Dobróka, M., Daróczi, L., and Beke, D. (2013). Effect of thermal and mechanical cycling on the elastic and dissipative energy in CuAl (11.5 wt%) Ni (5.0 wt%) shape memory alloy, *Journal of Alloys and Compounds*, C 577, S517-S520.

[62] Recarte, V., Perez-Landazabal, J., Rodríguez, P., Bocanegra, E., Nó, M., and San Juan, J. (2004). Thermodynamics of thermally induced martensitic transformations in Cu–Al–Ni shape memory alloys, *Acta Materialia*, C 52, 3941-3948.

[63] Saud, S.N., Bakar, T.A.A., Hamzah, E., Ibrahim, M.K., and Bahador, A. (2015). Effect of quarterly element addition of cobalt on phase transformation characteristics of Cu-Al-Ni shape memory alloys, *Metallurgical and Materials Transactions A*, C 46, 3528-3542.

[64] Dagdelen, F., Kok, M., and Qader, I. (2019). Effects of Ta Content on Thermodynamic Properties and Transformation Temperatures of Shape Memory NiTi Alloy, *Metals and Materials International*, C, 1-8.

[65] Umetsu, R., Ito, K., Ito, W., Koyama, K., Kanomata, T., Ishida, K., and Kainuma, R. (2011). Kinetic arrest behavior in martensitic transformation of NiCoMnSn metamagnetic shape memory alloy, *Journal of Alloys and Compounds*, C 509, 1389-1393.

[66] Zu, X., Wang, L., Huo, Y., Lin, L., Wang, Z., Lu, T., Liu, L., and Feng, X. (2002). Effect of electron irradiation on the transformation characteristics of narrow hysteresis TiNiCu shape memory alloys, *Applied Physics Letters*, C 80, 31-33.

[67] Greiner, W., Neise, L., and Stöcker, H., (2012). *Thermodynamics and statistical mechanics*, Springer Science & Business Media,

[68] Shiva, S., Palani, I., Mishra, S., Paul, C., and Kukreja, L. (2015). Investigations on the influence of composition in the development of Ni–Ti shape memory alloy using laser based additive manufacturing, *Optics & Laser Technology*, C 69, 44-51.

[69] Shakir, A.A., Abubakar, T., and Saud, S.N. *The Effect of Aging on the Transformation Temperatures and Microstructure of Cualni-Mn Shape Memory Alloys*. in *Journal of Physics: Conference Series*. 2018. IOP Publishing.

CURRICULUM VITAE

Name: Bahar Ali Mohammed FARAJ

Surname: FARAJ

Date of Birth: 01-Jun-1993

Place of Birth: Sulaymaneyah-Iraq

Email: baharali9931@gmail.com

Education Information:

- ✓ Graduated from University of Sulaymanyah (2011 - 2015) / Iraq

International Conference Presentations:

1) Ahmed Omar Ali Al-Jaf, F. Dagdelen, E. Ozen, M.Kok, ***Bahar Ali M.Faraj Roghzai***, Investigation of Thermal Cycles Behavior of NiTi-20 Ta Shape Memory Alloy, Oral Presentation, International Conference on Physical Chemistry and Functional Materials (PCFM'18), 2018
2) E. Ozen, M. Kok, F. Dagdelen, ***Bahar Ali M.Faraj Roghzai***, Ahmed Omar Ali Al-Jaf, Thermal Cycle Effects on Physical Properties of NiTi-20Nb Shape Memory Alloy, Poster presentation, International Conference on Physical Chemistry and Functional Materials (PCFM'18),2018